Pathogenic TRIO variants associated with neurodevelopmental disorders perturb the molecular regulation of TRIO and axon pathfinding in vivo

Maxime Bonnet, Fiona Roche, Christine Fagotto-Kaufmann, Gabriella Gazdagh, Iona Truong, Franck Comunale, Sonia Barbosa, Marion Bonhomme, Nicolas Nafati, David Hunt, et al.

Pathogenic TRIO variants associated with neurodevelopmental disorders perturb the molecular regulation of TRIO and axon pathfinding in vivo

Maxime Bonnet, Fiona Roche, Christine Fagotto-Kaufmann, Gabriella Gazdagh, Iona Truong, Franck Comunale, Sonia Barbosa, Marion Bonhomme, Nicolas Nafati, David Hunt, et al.

Pathogenic *TRIO* variants associated with neurodevelopmental disorders perturb the molecular regulation of TRIO and axon pathfinding in vivo

Maxime Bonnet[1], Fiona Roche[2], Christine Fagotto-Kaufmann[1], Gabriella Gazdagh[3,4], Iona Truong[1,14], Franck Comunale[1], Sonia Barbosa[1], Marion Bonhomme[1], Nicolas Nafati[5], David Hunt[6], Monserrat Pons Rodriguez[7], Ayeshah Chaudhry[8,9], Deborah Shears[10], Marcos Madruga[11], Fleur Vansenne[12], Aurore Curie[13], Andrey V. Kajava[1], Diana Baralle[3], Coralie Fassier[2], Anne Debant[1,15]✉ and Susanne Schmidt[1,15]✉

The RhoGEF TRIO is known to play a major role in neuronal development by controlling actin cytoskeleton remodeling, primarily through the activation of the RAC1 GTPase. Numerous *de novo* mutations in the *TRIO* gene have been identified in individuals with neurodevelopmental disorders (NDDs). We have previously established the first phenotype/genotype correlation in TRIO-associated diseases, with striking correlation between the clinical features of the individuals and the opposite modulation of RAC1 activity by TRIO variants targeting different domains. The mutations hyperactivating RAC1 are of particular interest, as they are recurrently found in patients and are associated with a severe form of NDD and macrocephaly, indicating their importance in the etiology of the disease. Yet, it remains unknown how these pathogenic *TRIO* variants disrupt TRIO activity at a molecular level and how they affect neurodevelopmental processes such as axon outgrowth or guidance. Here we report an additional cohort of individuals carrying a pathogenic *TRIO* variant that reinforces our initial phenotype/genotype correlation. More importantly, by performing conformation predictions coupled to biochemical validation, we propose a model whereby TRIO is inhibited by an intramolecular fold and NDD-associated variants relieve this inhibition, leading to RAC1 hyperactivation. Moreover, we show that in cultured primary neurons and in the zebrafish developmental model, these gain-of-function variants differentially affect axon outgrowth and branching in vitro and in vivo, as compared to loss-of-function TRIO variants. In summary, by combining clinical, molecular, cellular and in vivo data, we provide compelling new evidence for the pathogenicity of novel genetic variants targeting the *TRIO* gene in NDDs. We report a novel mechanism whereby the fine-tuned regulation of TRIO activity is critical for proper neuronal development and is disrupted by pathogenic mutations.

INTRODUCTION

Neurodevelopmental disorders (NDDs) such as autism spectrum disorders (ASD) and intellectual disability (ID) originate from disruption in the development of the nervous system, leading to altered brain function. NDDs are disorders with a significant genetic component and the advent of high throughput sequencing technologies has allowed the identification of an increasing number of genes that are found mutated in these pathologies [1]. However, despite intensive studies, the understanding of the pathophysiological mechanisms of these complex diseases is far from complete.

During brain development, neurons extend an axon that navigates through a complex environment to reach its final target. This process is required for establishing correct neuronal connectivity, essential for normal brain function. Axon outgrowth and guidance is driven by a specific, F-actin rich structure at the tip of the axon, called the growth cone, which senses and integrates the signal of extracellular guidance cues, translating it into actin cytoskeleton remodeling that ultimately produces motility and steering [2]. The dynamic F-actin network is concentrated in the peripheral domain of the growth cone, with

[1]Centre de Recherche en Biologie Cellulaire de Montpellier (CRBM), University of Montpellier, CNRS, Montpellier, France. [2]Institut de la Vision, Sorbonne University, CNRS, INSERM, Paris, France. [3]Faculty of Medicine, University of Southampton, Southampton SO16 5YA, UK. [4]Wessex Clinical Genetics Service, University Hospital Southampton National Health Service Foundation Trust, Southampton SO16 5YA, UK. [5]Montpellier Ressources Imagerie, BioCampus, University of Montpellier, CNRS, INSERM, 34293 Montpellier, France. [6]Wessex Clinical Genetics Service, Princess Anne Hospital, Southampton SO16 5YA, UK. [7]Hospital Universitari Son Espases, 07120 Palma, Illes Balears, Spain. [8]Department of Laboratory Medicine and Genetics, Trillium Health Partners, Mississauga, ON, Canada. [9]Department of Laboratory Medicine and Pathobiology, University of Toronto, Toronto, ON, Canada. [10]Oxford Centre for Genomic Medicine, Oxford University Hospitals NHS Foundation Trust, Oxford, UK. [11]Hospital Viamed Santa Ángela De la Cruz, Sevilla 41014, Spain. [12]Department of Clinical Genetics, University Medical Center, , Groningen, , 9713 GZ Groningen, The Netherlands. [13]Reference Center for Intellectual Disability from rare causes, Department of Child Neurology, Woman Mother and Child Hospital, Hospices Civils de Lyon, Lyon Neuroscience Research Centre, CNRS UMR5292, INSERM U1028, Université de Lyon, Bron, France. [14]Present address: Institut de Génomique Fonctionnelle (IGF), Université de Montpellier, CNRS, INSERM, Montpellier, France. [15]These authors contributed equally: Anne Debant, Susanne Schmidt. ✉email: anne.debant@crbm.cnrs.fr; susanne.schmidt@crbm.cnrs.fr

F-actin bundles forming filopodia separated by sheets of broad lamellipodia [3]. By their ability to regulate F-actin cytoskeleton remodeling, the Rho GTPases control key steps of nervous system development, including axon outgrowth and guidance [4].

The Rho Guanine nucleotide Exchange Factor (RhoGEF) TRIO is a well-established regulator of neuronal development by modulating neuronal migration, axon outgrowth/guidance and synaptogenesis through the activation of the GTPase RAC1 [5–7]. The constitutive knock-out of the *TRIO* gene in the mouse is embryonic lethal and leads to numerous defects in brain organization [8]. Targeted deletion of *TRIO* in the hippocampus and the cortex during early mouse embryogenesis results in progressive defects in the learning ability, sociability and motor-coordination in these mice [9, 10]. Together, these data show that TRIO is an essential gene for the development and function of the mammalian nervous system.

At the molecular level, TRIO's GEF activity towards RAC1 is carried by the GEFD1 domain, composed of a catalytic DH1 (Dbl-homology) domain and a regulatory PH1 (Pleckstrin-homology) domain, which assists the DH1 domain in its binding to the GTPase [11–13]. However, how TRIO activity towards RAC1 is regulated in the context of the full-length protein is not yet fully understood. Indeed, in addition to the GEFD1 domain, TRIO includes a second, RHOA-specific, GEF domain and many other protein domains, whose contribution to TRIO function is not well characterized. For example, the spectrin repeat region at the N-terminus of TRIO (hereafter called spectrin domain), has been proposed to participate in intramolecular folding of TRIO, which possibly leads to the inhibition of the catalytic GEFD1 domain [14]. Different studies have suggested that this intramolecular fold could be released by binding of the spectrin repeats to different proteins such as DISC-1, Kiddins220/ARMS and NAV1 [14–16], thus facilitating the access of RAC1 to GEFD1 and thereby promoting RAC1 activation. However, the precise molecular mechanism underlying this intramolecular folding is poorly understood.

Given the importance of TRIO in neurodevelopment, it is not surprising that whole exome sequencing studies have recently identified more than a hundred different *de novo* mutations in the *TRIO* gene in distinct cohorts of individuals with heterogeneous NDDs, including ASD and/or ID [17–24]. We have contributed to establishing TRIO as a novel monogenic cause for NDDs, reporting an important number of *de novo* mutations in *TRIO* that fall into two different clusters with two different phenotypic representations (i.e. the spectrin and GEFD1 domains) [22, 25]. The mutations in the 7th spectrin repeat domain (cluster 1) are associated with severe forms of ID and ASD and macrocephaly, and induce RAC1 hyperactivation. Mutations in the RAC1-specific GEFD1 domain (cluster 2) are associated to mild ID and microcephaly, and impair RAC1 activity. We proposed that deregulated modulation of RAC1 activity by TRIO variants may represent a pathogenic mechanism for these diseases. Indeed, depending on the nature of the mutation and the domain targeted, the mutations affect TRIO's activity towards RAC1 in opposite ways, which in turn causes distinct clinical disorders [25]. Yet, how these pathogenic TRIO variants affect neurodevelopmental processes such as axon outgrowth and guidance, which are controlled by TRIO and are essential for brain function, has not been investigated so far.

The mutations identified in cluster 1, which hyper-activate RAC1 and are associated with severe NDD and macrocephaly, are of particular interest. They have been found in an important number of unrelated individuals with a similar phenotype, reinforcing the contribution of these specific TRIO variants to the pathology. However, the molecular mechanisms by which this cluster of mutations leads to RAC1 hyperactivation are unknown, as the spectrin domain has no catalytic activity towards RAC1 per se, suggesting that an indirect mechanism is involved.

Here we report a cohort of 14 individuals carrying a pathogenic *TRIO* missense variant that allowed us to identify new mutations not only in the spectrin domain, but also in GEFD1, which lead to RAC1 hyperactivation and are associated with severe ID/macrocephaly. By performing conformation predictions coupled with biochemical validation, we propose a model wherein TRIO is inhibited under physiological conditions, and NDD-associated variants relieve this inhibition, explaining how pathogenic variants in the spectrin or GEFD1 domain can lead to RAC1 hyperactivation. In addition, we show that these gain-of-function TRIO variants differentially affect axon outgrowth and growth cone dynamics as compared to the loss-of-function TRIO variants of cluster 2. Interestingly, these gain-of-function TRIO variants similarly alter axon outgrowth/pathfinding in the zebrafish. These data provide the first in vivo evidence of the impact of these pathogenic TRIO variants on neuronal circuit development, and strengthen their potential contribution to the disruption of proper neuronal connectivity in the brain of affected individuals.

Taken together, our data provide new molecular insights into the regulatory modes of TRIO activity, how these could be disrupted under pathological conditions, and reveal how pathogenic TRIO variants affect key steps of neuronal development such as axon outgrowth/pathfinding. Finally, our current findings refine the phenotype/genotype correlation we had established previously [25] and clearly associate TRIO dysfunction to the etiology of these NDDs.

SUBJECTS, MATERIALS AND METHODS

Identification of pathogenic TRIO variants and patient consent

TRIO gene variants were identified through diagnostic clinical practice either through panel, exome, or genome testing. Variants were reported according to standardized nomenclature defined by the reference human genome GRCh37 (hg19) and TRIO transcript GenBank: NM_007118. None of the missense variants were listed in gnomAD.

Patient consent for participation and phenotyping was obtained through the referring clinical team. Consent and collection of information conformed to the recognized standards of the Declaration of Helsinki.

Molecular modeling of TRIO domains

Modeling of the TRIO/RAC1 complex was undertaken by using (1) a structural model of the TRIO fragment 894-1587 made by AlphaFold [26]. Complex (2) was modeled with the crystal structures of DH1 (PDB: 1NTY) and the complex with RAC1 (PDB: 1KZ7). The complex of the TRIO fragment 894-1587 with the small GTPase substrate RAC1 was obtained by superposition of DH1 domain from model (1) and (2). Figures of the protein structures were generated with PyMol.

For the TRIO modeling in Figs. 2 and 3, we used the Drosophila TRIO (isoform A) structure prediction, available in the AlphaFold Protein Structure Database. Blue regions indicate a very high model confidence index (per-residue confidence score (pLDDT) > 90), cyan indicate a high confident index (90 > pLDDT > 70), yellow indicate a low confidence index (70 > pLDDT > 50) and orange indicate a very low confidence index (pLDDT< 50). This conformation prediction is freely available on https://alphafold.ebi.ac.uk.

Plasmids, DNA constructs

The pEGFP-TRIO and pEGFP-TRIO GEF-dead constructs have been described previously [16, 27]. All missense and non-sense mutants were generated with the QuikChange Site-directed mutagenesis kit (Agilent Technologies) according to the manufacturer's instructions, using appropriate primers. The double mutant R1078W-GEFdead (GD) was generated by introducing Q1427A and L1435E mutations into GEFD1, using the same QuikChange Site-directed mutagenesis kit. Primer sequences are available upon request, and all constructs were verified by sequencing. The

pLifeact-mTurquoise (Lifeact-Tq) plasmid was kindly provided by J. Goedhart (University of Amsterdam, The Netherlands).

Antibodies

List of all primary antibodies used: for immunoblotting, phospho-Ser144 PAK antibody (rabbit; Cell Signaling, #2606S, 1/1000), PAK1 antibody (mouse; Santa Cruz sc-166887, 1/1000), GFP antibody (rabbit; Torrey Pines Biolabs, #TP401, 1/3000), RAC1 antibody (mouse; BD Biosciences 610651, 1/1000); for immunocytochemistry, anti-GFP (chicken, Aves Labs, 1/1000), anti-MAP-2 (Santa Cruz, 1/500). List of all secondary antibodies used: Dylight Rabbit 680 (Thermo Fisher Scientific, 35568), Dylight Mouse 800 (Thermo Fisher Scientific, SA5-35521), Alexa Fluor 488 anti-chicken (Thermo Fisher Scientific, A11039), Alexa Fluor 633 anti-mouse (Thermo Fisher Scientific, A21050), Phalloidin TRITC (Sigma-Aldrich, P1951, 1/40,000), Hoechst (Sigma-Aldrich, B2261, 1/50,000).

Cell culture, transfection and immunoblot analysis of Phospho-PAK amounts

HEK293T and N1E-115 neuroblastoma cell lines were obtained from ATCC and were regularly tested for mycoplasma contamination by PCR. Cells were cultured and transfected as described in [25]. Immunoblot analysis for quantification of Phospho-PAK levels were also performed as described in [25], as was the quantification of lamellipodia in N1E-115 cells.

RAC1^{N17} binding assay

The TRIO-RAC^{N17} binding assays were performed as described in [25]. Briefly, HEK293T cells were co-transfected with the indicated biotinylated GFP-TRIO or GFP-GEFD1 variants and a pLXSN-Myc-RAC1^{N17} plasmid. We used the RAC1^{N17} construct, which is a dominant negative form of RAC1 that mimics the GDP-bound form of the GTPase and thus binds the GEF with higher affinity than WT RAC1. Forty-eight hours post transfection, cells were lysed (for lysis buffer see [25]). TRIO was pulled down with Streptavidin Dynabeads (Dynabeads M-280 Streptavidin Invitrogen), and co-precipitating RAC1^{N17} was detected by immunoblotting with a RAC1 antibody. Total cell lysates were analyzed with RAC1 and GFP antibodies.

Streptavidin-based pull-down assays

Protein extract preparation and pull-down experiments were carried out as described [16]. Briefly, HEK293T cells were transfected with biotinylated TRIO constructs (bGFP, bGFP-Spectrin Repeat (SR) wt or bGFP-Spectrin Repeat (SR) R1078W) together with GFP-tagged TRIO (or GFP alone as control). Forty-eight hours post transfection, cells were lysed, and the biotinylated proteins were pulled down with streptavidin Dynabeads. After extensive washing, interacting proteins were resolved by SDS-PAGE and immunoblotted with an anti-GFP antibody.

Animal care and maintenance

Wild-type RjOrl:Swiss pregnant female mice (Janvier Labs, St Berthevin, France), used for generating E17.5 embryos for primary cultures of hippocampal neurons, were housed at the animal house facility of the Institut de Génétique Moléculaire de Montpellier (Montpellier, France). Animals had a libitum access to food and water, with 12h-light-dark cycle. The mouse facility has been approved by the Département des pratiques de recherche réglementées " Animaux à des fins scientifiques" – AFiS, under the approval number F3417216.

Zebrafish embryos (*Danio rerio*) were obtained from natural spawning of Tg (*HuC*:GAL4) [28] transgenic fish. All embryos were maintained at 28 °C in E3 medium (5 mM NaCl, 0.17 mM KCl, 0.33 mM $CaCl_2$, 0.33 mM $MgSO_4$, 0.00001% (w/v) Methylene Blue) and staged by hours post-fertilization (hpf) and gross morphology according to [29]. To prevent pigment formation, 0.2 mM of 1-phenyl-2-thiourea (PTU, Sigma) was added to the E3 media from 24 h post-fertilisation (hpf) onwards. All experiments were made in agreement with the European Directive 210/63/EU on the protection of animals used for scientific purposes, and the French application decree 'Décret 2013-118'. The fish facility has been approved by the French 'Service for animal protection and health', with the approval number A-75-05-25. Zebrafish experiments were conducted on embryos/larvae younger than 5 days post fertilization, which are capable of independent feeding and are not protected by ethical statements. In the zebrafish, sexual determination is influenced by genetic and environmental factors and occurs between 21–23 days post fertilization. Prior, all zebrafish develop ovary-like gonads, regardless of their chromosomal background. Accordingly, our functional analysis of motor neuron axon pathfinding in 72-hpf transgenic larvae have been conducted under gender-free consideration.

Generation of UAS-TRIO-GFP-CAAX constructs and transient transgenesis in the zebrafish

cDNAs encoding human WT or pathogenic variants of TRIO (R1078Q, R1078W and R1428Q) and a T2A cleavable peptide fused to a membrane-targeted GFP (T2A-GFP-CAAX) were PCR amplified from pEGFP-TRIO plasmids, using the CloneAmp HiFi PCR Premix (Ozyme, France) and the following primers:

- *TRIO_FOR*: 5′-tcttctcagcgtaaagccac CATGAAAGCTATGGATGTT TTAC-3′
- *TRIO_REV*: 5′- ctccgccgccAACTCTAGGCAGAAGCCTG-3′

Each TRIO cDNA was subsequently cloned in fusion with a T2A-GFP-CAAX cDNA (synthesized by GeneCust, France) in a Nhe-I linearized *pUAS:ubc-pA* backbone containing a 14xUAS-E1b promoter, a UbC intron and tol1 sites [30] (kind gift of the Del Bene lab, Institut de la Vision, Paris), using the NEBuilder® HiFi DNA Assembly Cloning kit (New England Biolabs, UK).

Mosaic expression of WT or pathogenic variants of TRIO in zebrafish developing motor neurons was achieved by injecting 1-cell stage Tg(*HuC*:GAL4) transgenic embryos with a solution containing 40 ng/µl of *UAS*:TRIO-T2A-GFP-CAAX plasmids and 40 ng/µl of Tol1 transposase mRNAs. Injected larvae were screened and sorted at 48hpf for normal trunk development and GFP expression in motor neurons and then fixed at 72-hfp for analysis. Due to the low efficiency of transient transgenesis with the *UAS*:TRIO-T2A-GFP-CAAX constructs and the high degree of mosaicism in SMN-targeted TRIO expression in transgenic embryos, we chose to inject more than 200 one-cell stage embryos with each TRIO construct to get more than 50 GFP+ SMNs—from at least 20 larvae—per TRIO variant for robust statistical analyses.

In toto immunolabelling on zebrafish larvae

Zebrafish transgenic embryos were fixed at 72-hfp in PBS/4% paraformaldehyde for 2 h at room temperature, washed 3 times with PBST 1% (1% Triton X-100 in PBS) and permeabilised for 14 min with a 0.25% trypsin solution (Gibco) at 25 °C. Embryos were then blocked for 2 h in PBST 1% supplemented with 10% normal goat serum and incubated overnight at 4 °C with Zn-5 (1/150; ZIRC, University of Oregon) and GFP (1/1000; Molecular Probes) antibodies diluted in PBST 1%/1% normal goat serum. After several washes in PBST 1%, embryos were incubated overnight at 4 °C with the appropriate secondary antibody (Alexa Fluor 488 and 555 at 1/1000, Molecular Probes). Images were acquired using a fluorescence microscope equipped with an Apotome module (Zeiss, Axiovert 200 M), a 20x objective (NA 0.5), the AxioCam MRm camera (Zeiss) and the Axiovision software (Zeiss). Images were processed with the NIH Image J software. Each figure panel corresponds to a projection image from a z-stack of 2-µm sections. Quantification of the impact of TRIO variant overexpression on ventrally projecting CaP-like axons was performed by measuring the length of GFP+ axons (i.e. from their

spinal cord exit point to their distal tip) normalized to the length of non-transgenic neurons (i.e. GFP-negative and zn-5 positive axons).

Primary neuronal culture and transfection and reagents

Hippocampal neurons from E17,5 mice embryos were dissociated mechanically and plated on Poly-L-Ornithine (0,25 mg/ml)-coated coverslips in 6-well dishes at a density of 250,000 cells/well (adapted from [31]). Neurons were transfected at DIV1 with cDNA constructs as indicated, using Lipofectamine 2000 transfection reagent (Thermofisher) according to manufacturer's instructions. During transfection, neurons were placed into Neurobasal medium (Gibco) supplemented with B27 (Gibco, 1×), Glutamax (Gibco, 1×), penicillin/streptomycin (5 µg/ml). After transfection, the medium was replaced by the conditioned medium (containing glucose).

In vitro Immunolabelling and quantification

Hippocampal neurons (DIV3) were fixed with 4% paraformaldehyde/4% sucrose in PBS for 10 min and permeabilized in 0.15% Triton-X-100/PBS for 3 min. Immunostaining was performed with the indicated primary antibodies and the corresponding Alexa Fluor 488 or 633-congugated secondary antibodies (Thermo Fisher Scientific). All coverslips were mounted with the Prolong Gold Antifade reagent (Invitrogen).

For neurite morphology quantifications, images were acquired using a fluorescence microscope (Zeiss Axioimager Z2) and a 20× objective (NA 0.8). We considered as a neurite the processes with a length at least equal to the diameter of the soma, and we measured the length of the longest neurite of each single neuron. For the quantification of neurite branching, we counted the number of MAP-2-positive collaterals emerging from a single neurite, among all the neurites emerging from the soma. The quantification of the growth cone perimeter and the number of filopodia in the growth cone were assessed by actin staining (phalloidin), and were done using the ImageJ software.

For growth cone shape representation, growth cones ROIs were plotted using the "Growth-Cone-Visualizer" ImageJ macro (Github.com/Montpellier Ressources Imagerie).

Live-imaging and quantification

Hippocampal neurons were plated in IBIDI glass-bottom dishes at the density of 150,000 cells/well. Neurons were co-transfected (DIV1) with TRIO constructs and Lifeact-Tq, and video-microscopy was performed at DIV3 by using a Spinning Disk Nikon TI Andor CSU-X1, equipped with a 100× objective (NA 1.45). To visualize F-actin dynamics, Lifeact-Tq in co-transfected neuronal growth cones was imaged during 2 min (2 images/s). Filopodia extension and retraction events were quantified by manual tracking and characterized by a forward or backward movement, respectively, that progresses during at least two consecutive frames without pauses.

Statistical analysis

Statistical analyses for immunoblots of phospho-PAK levels (Figs. 1–3), TRIO/RAC pulldown (Fig. 3) and Spectrin/TRIO co-pulldown assays (Supplement Fig. 1) were made by non-parametric one-way ANOVA, Kruskal–Wallis test and Dunns' post-test. Asterisks indicate datasets significantly different from WT ($*p < 0.05$, $**p < 0.01$, $***p < 0.001$). All data were obtained from at least 5 independent experiments and are shown as mean ± S.E.M.

Statistical analyses of neuronal morphology changes were made by one-way ANOVA, Dunnett test ($*p \le 0.05$; $**p \le 0.01$; $***p \le 0.001$). Data were obtained from at least 5 independent experiments of neuronal cultures: a total of 77 GFP, 78 TRIO-WT, 44 TRIO-R1078W, 61 TRIO-R1078Q, 45 TRIO-E1299K and 55 TRIO-R1428Q expressing neurons were analyzed. Statistical analyses of actin dynamics were made by One-way ANOVA, Dunnett test ($*p \le 0.05$; $**p \le 0.01$; $***p \le 0.001$). Data were obtained from a total of 28 GFP, 26 TRIO-WT, 15 TRIO-R1078W, 27 TRIO-R1078Q, 11 TRIO-E1299K and 26 TRIO-R1428Q expressing neurons.

For the zebrafish studies: All data were obtained from at least three independent experiments. Morphometric analyses and quantifications were blindly done (no randomization was used). For SMN neurons: a total of 219 WT, 55 R1078W, 156 R1078Q and 118 R1428Q positive SMNs were included in these quantifications. For CAP-like neurons: quantifications were carried out on 71 TRIO-WT, 34 TRIO-R1078W, 113 TRIO-R1078Q and 63 TRIO-R1078W CaP-like neurons observed in 29, 15, 23 and 30 transgenic embryos respectively. The statistical significance of the data was evaluated using the non-parametric Kruskal–Wallis ANOVA test with Dunn's post-test when comparing more than two groups assuming non-Gaussian distribution. Data distribution was tested for normality using the D'Agostino and Pearson normality test. The Chi-square test (χ^2 test) was used to assess the statistical distribution of the motor neuron phenotypes observed between the different TRIO constructs. All Statistical analyses were performed using GraphPad Prism 5.00 (GraphPad Software, San Diego, CA).

RESULTS

Identification of new TRIO variants associated to severe NDD and causing RAC1 hyperactivation

TRIO variants clustering in the spectrin domain (cluster 1) are of particular interest as they are associated to severe NDD and macrocephaly in a recurrent number of unrelated individuals, and lead to hyperactivation of RAC1 [25]. We therefore aimed to identify new variants in the *TRIO* gene that could reinforce this genotype/phenotype correlation. To this end, we analysed the clinical phenotype of a new set of individuals carrying a confirmed pathogenic *de novo* missense variant in the *TRIO* gene and presenting with neurodevelopmental delay. The mutations were clustered into three main groups. The variants of the first group (individuals 1–8) target five adjacent amino acids that are highly conserved across evolution and fall within the cluster 1 variants we previously identified [25] (Fig. 1A, Supplementary Fig. 1A and Table 1). Of note, T1075I and R1078W variants had already been found in patients in our previous study. Arg1078 is to date the most frequently found mutated amino acid in *TRIO* in individuals with NDDs, with 12 unrelated patients harboring this mutation, including 4 in this cohort. Within group 1, we delineate a consistent phenotype of severe intellectual disability and macrocephaly, confirming the phenotype/genotype correlation that we established previously (Table 1 and [25]).

A second group of mutations, comprising variants identified in patients 9–11 (Leu1124Ser, Val1141Met and Glu1159Lys), all lie on an α-helix immediately adjacent to the α-helix targeted by group 1 mutations and also affect highly conserved residues (Supplementary Fig. 1A). In contrast to group 1 individuals, the clinical features of these individuals are more heterogeneous (Fig. 1A and Table 1).

A third group of individuals (12–14) carry missense mutations on conserved residues within the RAC1-activating GEFD1 domain (Supplementary Fig. 1B). Variants Asp1368Val, His1371Tyr have already been described elsewhere [23, 32]. The GEFD1 domain has previously been identified as a mutational hotspot in *TRIO* [22, 23, 25, 33]. Of note, most of the mutations within this domain, with the notable exception of Asp1368Val, were so far described as loss-of-function variants, leading to decreased GEFD1-mediated RAC1 activation and were associated to microcephaly and milder ID in patients. In contrast, the three variants listed here (Asp1368Val, His1371Tyr and Gly1448Arg) are located outside the α-helices (α1, α5, α6) known to be important for making direct contact with the RAC1 GTPase and hence for activating RAC1 (Supplementary Fig. 1B). Intriguingly, the phenotypes of the patients carrying these three variants are more severe

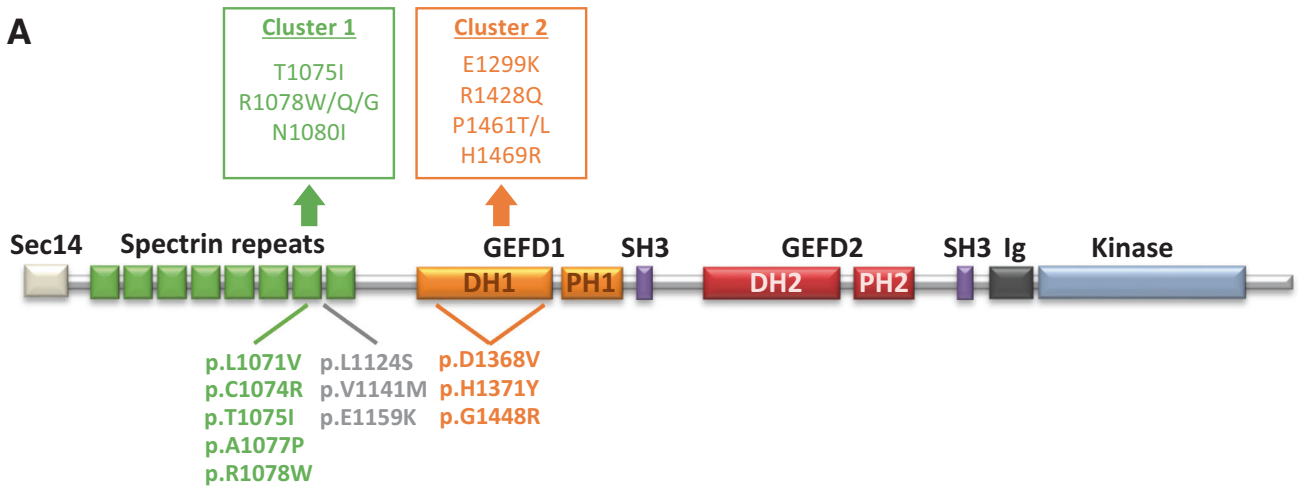

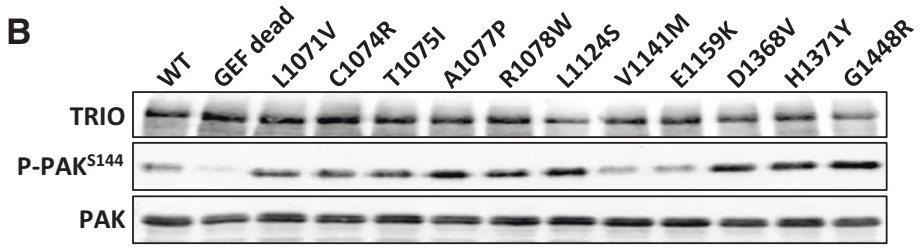

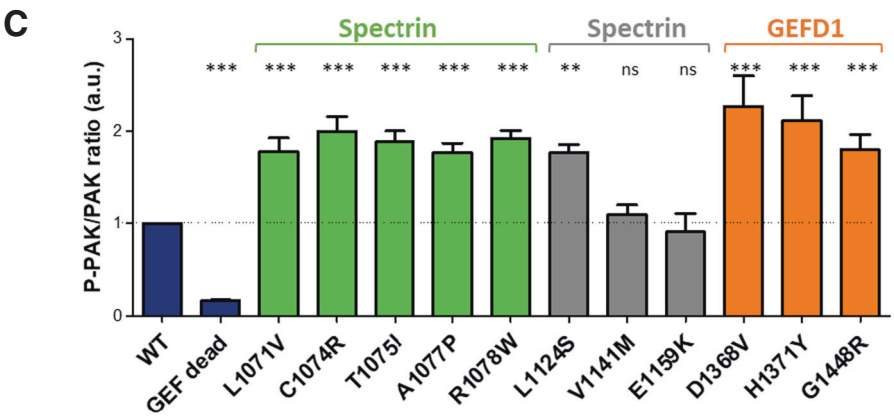

Fig. 1 Impact on RAC1 signaling of newly identified TRIO variants associated to neurodevelopmental disorders. A Schematic representation of the TRIO protein subdomains, and of the position of the clustered pathogenic variants studied. Above the protein are shown the previously reported variants of cluster 1, affecting the spectrin 7 repeat, and of cluster 2, targeting GEFD1 [25]. Below the protein are represented the new variants of this study. Five pathogenic variants, among which 3 were targeting new residues have been identified in spectrin 7 repeat (green), related to cluster 1, while 3 additional variations in the spectrin domain (gray) have been found, adjacent to cluster 1. Three new variants have been added to cluster 2 (orange). **B** Representative immunoblots of HEK293T cell lysates transfected with the indicated GFP-TRIO variants and detected with an anti-GFP antibody. GEF-dead is a TRIO form mutated in its GEF domain and unable to activate RAC1. PAK1 phosphorylation and total levels are detected with PAK1 antibodies, recognizing phosphorylated PAK on Ser144 or total PAK, respectively. **C** Quantification of the ratio of phospho-PAK1 levels over total PAK1 expression of the experiments performed in B. PAK1 phosphorylation measurement is used as a readout of the activation of the RAC1 signaling cascade. Quantifications were obtained from at least six independent experiments.

and associated to macrocephaly, resembling the phenotype of cluster 1 patients (Fig. 1A and Table 1).

We next tested the effects of all the newly identified variants on the main known function of TRIO, i.e. activation of the RAC1 signaling pathway. To do so, we monitored the effect of the different TRIO mutants on the phosphorylation levels of PAK1 as a readout of RAC1 activation, as described previously [25]. As shown in Fig. 1B, C, all the variants in group 1 led to hyperphosphorylation of PAK1. This is in line with the results we obtained previously, and significantly expands the number of variants found in cluster 1 and associated with a severe phenotype and macrocephaly in patients. Surprisingly, RAC1 hyperactivation

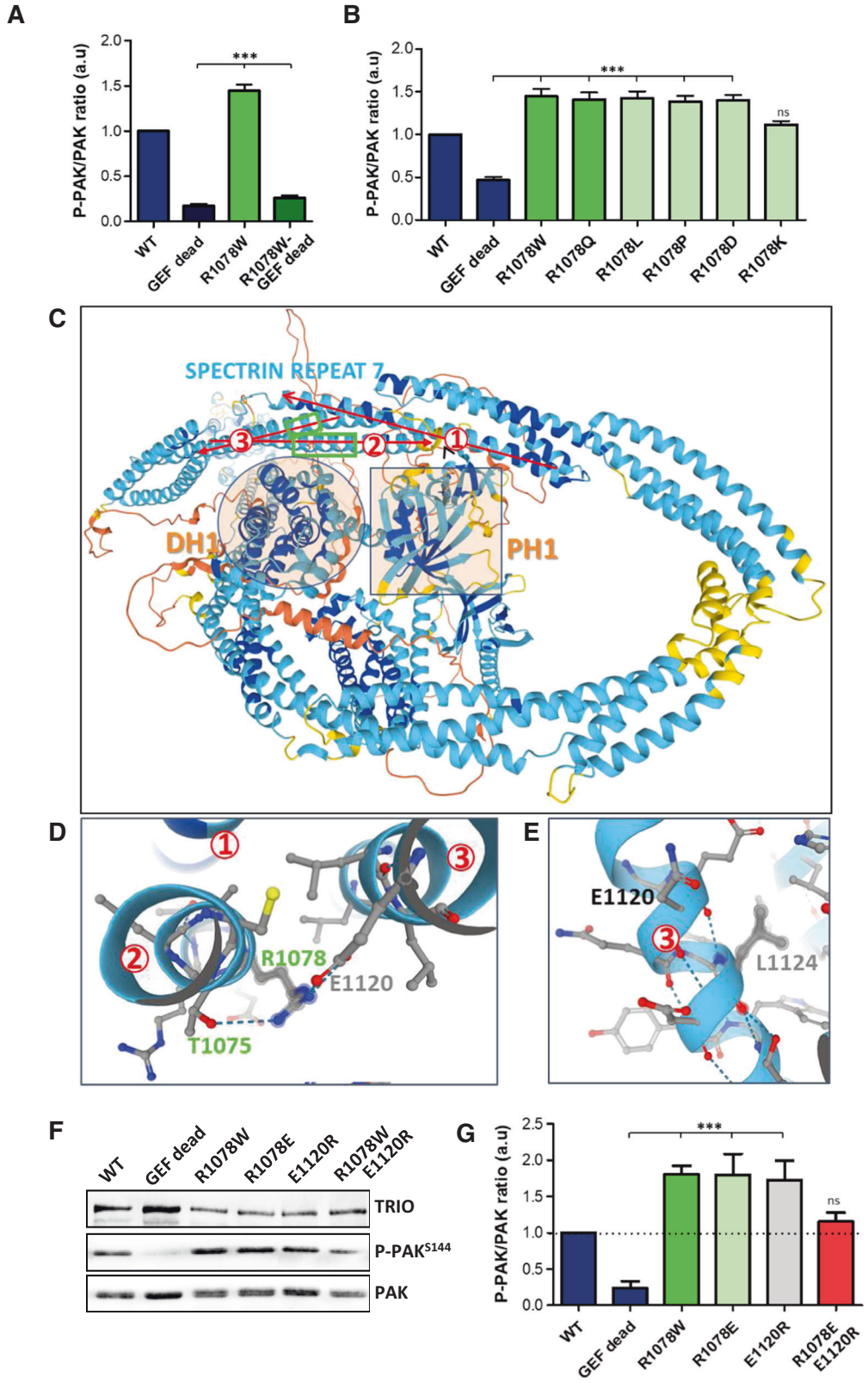

was also observed in cells expressing the Leu1124Ser variant, which is also located in the spectrin domain, but further downstream in the sequence. In contrast, the two other variants within this group (Val1141Met and Glu1159Lys) had no effect on RAC1 activation as compared to WT TRIO (Fig. 1B, C). Of note, none of the variants within group 2 are associated to macrocephaly in patients. The last group of variants, targeting the GEFD1 domain, all fell within cluster 2, wherein most of the variants had previously been shown to negatively affect RAC1 activity, like for example variants E1299K and R1428Q [25]. In contrast, the mutants

Fig. 2 Structural modeling reveals intramolecular interactions within the TRIO spectrin domain that are altered in pathogenic variants from cluster 1. A, B The positive charge of the Arginine 1078 is required for normal RAC1 activation. Quantification of the ratio of phospho-PAK1 levels over total PAK1 expression, measured from cell lysates of HEK293T cells transfected with the indicated GFP-TRIO mutants, as in Fig. 1. **C** Alphafold structure prediction showing the 3D conformation of the TRIO protein. The TRIO isoform A of Drosophila TRIO is presented, since it is the only sequence available in the Alphafold Protein Structure Database. The 7th spectrin repeat is composed of 3 helices (red circled numbers 1, 2 and 3). Green squares delineate the two regions in the 7th spectrin repeat that contain the amino acids targeted by the mutations and that are close spatially to the DH1 domain of the GEFD1. DH1 and PH1 domains of TRIO are shaded in orange. Zoom in the Alphafold prediction, showing an axial view of the triple helices of the 7th spectrin repeat (**D**) and a lateral view of helix 3 (**E**). The numbers of the helices correspond to those in **C** . Dotted blue lines, between residues R1078 and T1075, between R1078 and E1120 and between E1120 and L1124, represent predicted bonds between the amino acids. **F** Representative immunoblots of cell lysates of HEK293T cells transfected with the indicated artificial GFP-TRIO variants and detected with an anti-GFP antibody. PAK1 phosphorylation and total PAK levels are detected with PAK1 antibodies, against phosphorylated PAK on Ser144 or total PAK, respectively. **G** Quantification of phospho-PAK1/total PAK1 expression ratio. Quantification was obtained from at least five independent experiments.

Asp1368Val, His1371Tyr and Gly1448Arg all led to PAK hyperphosphorylation (Fig. 1B, C). Interestingly, all three individuals also presented with severe ID and macrocephaly, similarly to the patients in group 1, whose variants also caused RAC1 hyperactivation.

In conclusion, we have identified a number of new variants over-activating RAC1, not only in the previously described cluster 1, but also in other regions of the TRIO sequence. Most of the cases were associated with severe developmental delay and macrocephaly (Table 1), which reinforces the previously established genotype/phenotype correlation, and the association of TRIO dysfunction to the etiology of these NDDs.

Intramolecular interactions within the TRIO spectrin domain prevent TRIO-induced RAC1 activation, and these are disrupted by cluster 1 pathogenic variants

Given the increasing importance of these activating TRIO variants for NDD pathology, we sought to better understand how they affect TRIO activity at the molecular level. We were intrigued to understand how the mutations in cluster 1 led to a RAC1 hyperactivation, although the spectrin repeat domain has no catalytic GEF activity per se. To test whether this over-activation of RAC1 was dependent on the GEFD1 activity of TRIO, we introduced a GEF-dead mutation in the R1078W variant (TRIO-R1078W-GEF dead) and measured its ability to activate RAC1. As shown in Fig. 2A, the mutation abolishing GEFD1 activity completely abrogated PAK1 hyperphosphorylation induced by TRIO-R1078W, demonstrating that the observed overactivation of RAC1 was mediated by, and required a functional GEFD1 domain.

We further noticed that, in the pathogenic mutations affecting residue R1078, the basic Arginine amino acid was systematically replaced by non-basic amino acids, such as a Glutamine (R1078Q), a Tryptophan (R1078W) or a Glycine (R1078G) [25]. We therefore speculated whether the Arginine as such was important for normal RAC1 activation by TRIO, or whether it was its positive charge that was particularly important. We thus generated several artificial TRIO variants and assessed their ability to activate RAC1 by monitoring PAK1 phosphorylation levels (Fig. 2B) and lamellipodia formation in N1E-115 cells (Supplementary Fig. 1C), which represents another, cellular readout for RAC1 activation [25]. We showed that all the artificial mutants induced increased RAC1 activation and lamellipodia formation, except for the only positively charged R1078K mutant, which activated RAC1 and lamellipodia formation to similar levels as did WT TRIO. These data indicate that the positive charge associated to the Arginine is important for a normal TRIO-mediated RAC1 activation.

To further study the molecular mechanisms underlying the contribution of the spectrin domain to TRIO function, we turned to structural modeling. Thanks to recent progress in structure prediction achieved with the AlphaFold software [26], we could further deepen our prediction of the TRIO conformation. Due to the large size of the TRIO protein, the only TRIO sequence available so far in the AlphaFold Protein Structure Database is the Drosophila TRIO sequence. Nevertheless, as illustrated in Supplementary Fig. 1A, B, the sequence of TRIO is highly conserved between these two species, especially in the regions of interest to our study (40% overall identity, >60% identity in the GEFD1 domain). Using the Alphafold prediction tool, we first confirmed that each spectrin repeat is formed by a bundle of three entangled α-helices, as we had proposed previously [25], and that together, these 8 repeats of triple-helices seem to form a ring surrounding the GEFD1 and GEFD2 domains, which are grouped in the center of the structure (Fig. 2C).

The software further predicted that the 5 amino acids of cluster 1 are all located on the second helix of the triplet in the 7th spectrin repeat. Interestingly, the software predicted several interactions between them, most notably the tight bond between the R1078 and the T1075 residues, the latter being located only one helix-turn away (Fig. 2D). Given that these amino acids, when mutated in patients, led to a similar phenotype and to RAC1 hyperactivation, this supports the hypothesis that disrupting the interaction between these amino acids would have strong consequences on the three-dimensional structure of spectrin 7 repeat, and thus on TRIO function.

In addition to the intra-helical interaction R1078/T1075, the AlphaFold software also predicted that the positively charged R1078 most likely forms an ionic bond with the negatively charged Glutamic acid E1120, located on the adjacent third helix of the same bundle of helices (Fig. 2D). It is noteworthy that the E1120 residue in turn makes close contact with the L1124 residue in the same α-helix (Fig. 2E), which has been found mutated in patient 9 presenting with a severe phenotype, and which also led to RAC1 hyperactivation (Fig. 1B, C). This reinforces the importance of the interaction between the 2nd and the 3rd helix in the helix bundle. We suspected that disruption of the ionic bond between R1078 and E1120 by mutations would lead to the de-structuring of the helix bundle and thus of the whole 7th spectrin repeat. To test this hypothesis, we assessed the effect on TRIO-mediated RAC1 activation of artificial mutants of both amino acids, with the positively charged R1078 changed into a Glutamic acid (R1078E), and the negatively charged E1120 into an Arginine (E1120R). Figure 2F, G shows that, as expected, the R1078E variant strongly induced RAC activation. Interestingly, the E1120R variant also strongly over-activated RAC1, to the same extent as the R1078W mutant, suggesting that the change made in this residue contributed to the de-structuring of the helices. We then reasoned that we could restore the ionic bond, and hence the normal RAC activity, by swapping both charges in the same construct. We thus generated the double mutant R1078E/E1120R and showed in our PAK phosphorylation assays that this double mutant completely restored RAC1 activation to normal, wild-type levels (Fig. 2F, G). These findings demonstrate that the strong ionic bond between R1078 and E1120 is crucial for a proper folding of the spectrin 7 helix bundle, and thus for proper TRIO-mediated RAC activation.

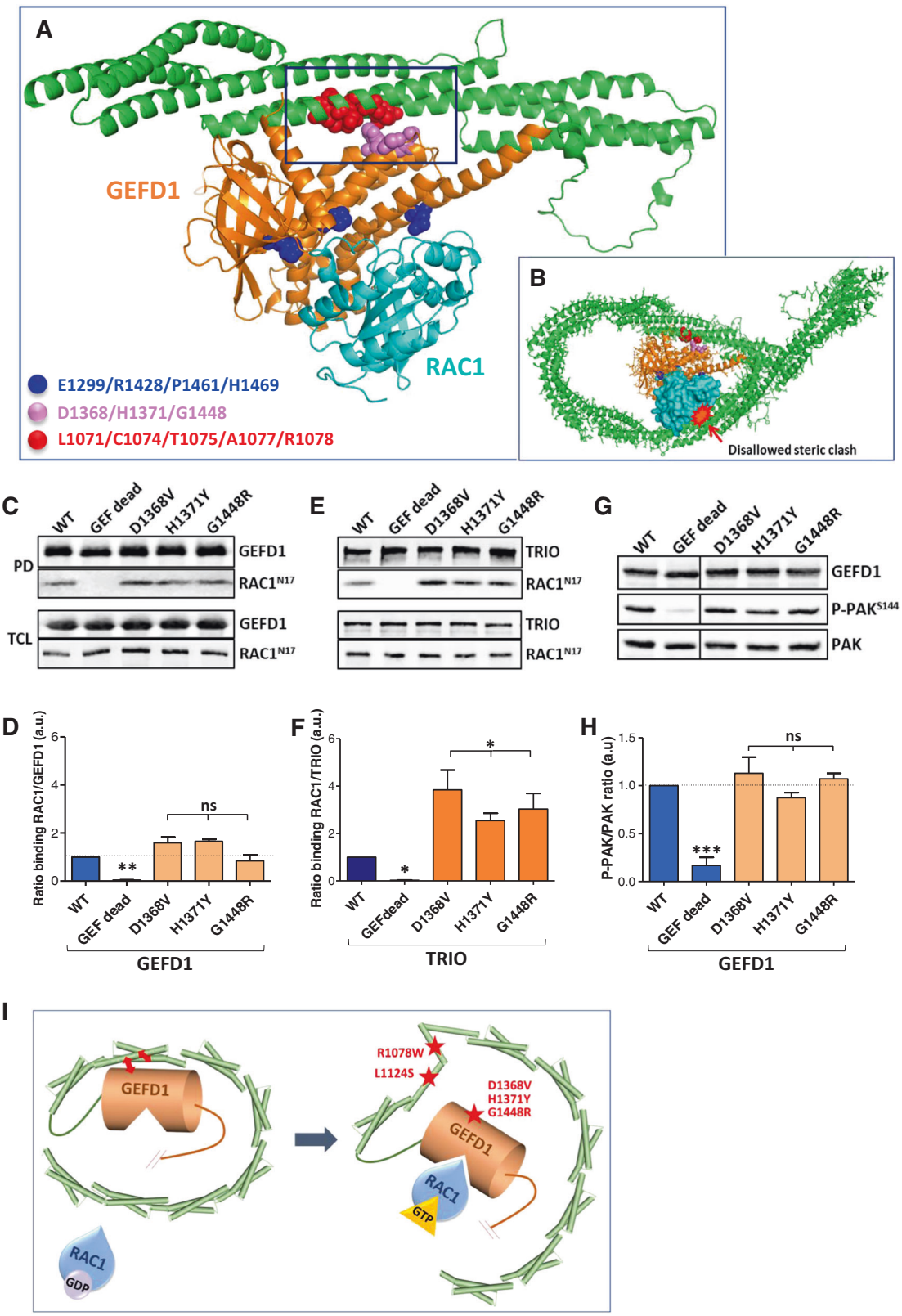

Molecular mechanisms by which pathogenic variants targeting either 7th spectrin domain or GEFD1 residues increase TRIO activity

By superimposing the conformational prediction of the 7th spectrin repeat/GEFD1 provided by AlphaFold and the known crystal structure of the GEFD1 domain in complex with RAC1 [12], we found that the DH1 domain, consisting mainly of 6 α-helices, was located in close proximity to the 2nd helix of Spectrin 7, carrying amino acids L1071 to R1078 (Fig. 3A, red residues). Interestingly, the residues of DH1 facing this spectrin helix (Fig. 3A,

Fig. 3 Molecular mechanisms by which pathogenic variants targeting either 7th spectrin domain or GEFD1 residues increase TRIO activity. A Structure prediction of the spectrin domain (green) and GEFD1 (orange) of TRIO in complex with RAC1 (cyan). Residues located at the interface between the DH1 domain of TRIO and the small GTPase RAC1 are in blue (E1299, R1428, P1461 and H1469) (see also Fig. 3 in [25]). Spectrin 7 residues of cluster 1 (red) are located in close proximity to the GEFD1 residues of cluster 2 (purple). The complex of the TRIO fragment 894-1587 with the small GTPase substrate RAC1 was obtained by superposition of DH1 domain from model (1) and (2). Figures of the protein structures were generated with PyMol. The residues D1368, H1371 and G1448 in the DH1 helices are facing the 5 residues (L1071, C1074, T1075, A1077, R1078) in the spectrin domain. **B** Structural model of TRIO (in its closed conformation) and the predicted position of the RAC1 GTPase, showing the disallowed steric clash with the folded spectrin helices. **C, E** Immunoblot analysis of the pulldown of the indicated TRIO GEFD1 (**C**) or full-length TRIO (**E**) constructs bound to $RAC1^{N17}$. Interacting proteins were resolved by SDS-PAGE and immunoblotted with a GFP antibody. PD: pulldown; TCL: total cell lysate. **D, F** Quantification of the binding of TRIO GEFD1 or full-length TRIO variants to $RAC1^{N17}$ in comparison with their respective WT counterparts. Quantification was obtained from three independent experiments. **G** Immunoblot analysis of HEK293T cells transfected with the GEFD1 domain of TRIO containing the mutations as indicated, and detected with an anti-GFP antibody. PAK1 phosphorylation amounts are detected with PAK1 antibodies, against phosphorylated or total PAK. **H** Quantification of the ratio of phospho-PAK1 amounts over total PAK1 expression, after expression of the different GEFD1 constructs. Quantification was obtained from at least four independent experiments. **I** Working model depicting how TRIO folding is relieved by pathogenic TRIO mutations. Pathogenic TRIO variants associated to neurodevelopmental disorders have served in proposing an interesting working model for the regulation of TRIO activity. Under physiological conditions, we propose that there is an inhibition of TRIO by intramolecular folding of its 7th spectrin domain onto its GEFD1 domain, preventing the access of GEFD1 to RAC1. The stretch of residues L1071 to R1078 in the 7th spectrin domain is most probably engaged both in an intramolecular binding to the GEFD1 domain, and in the stabilization of the 7th spectrin repeat, by making an interaction with E1120 in the adjacent alpha-helix. Pathogenic variants targeting the 7th spectrin domain or the DH residues would then relieve this inhibition, allowing better access of GEFD1 to RAC1, which might explain how the pathogenic TRIO variants lead to RAC1 hyperactivation.

purple residues) were precisely those found mutated in patients with severe ID and causing RAC1 hyperactivation (i.e. D1368V, H1371Y and G1448R). Intriguingly, these variants are situated at the opposite of the GTPase binding region, suggesting that they are not directly involved in GTPase binding and activation. This contrasted with our previously identified variants in DH1 (E1299K, R1428Q, P1461T and H1469R), leading to RAC hypoactivation and associated with microcephaly, which were all located at the interface with the GTPase in helices α1, α5, and α6 (Fig. 3A, blue residues). We had shown earlier that these variants were all affected in their ability to bind RAC1 and hence to activate it [25].

The observation that DH1 residues D1368, H1371 and G1448 were facing spectrin 7 residues L1071 to R1078, suggested an interaction between DH1 and spectrin repeat 7 (Fig. 3A). This prediction is consistent with the previously reported interaction between spectrin domains and GEFD1 [14]. We also found that the isolated TRIO spectrin repeats (SR) interact with the full-length TRIO protein (Supp Fig. 1D). Interestingly, this interaction was significantly reduced when using the isolated spectrin repeats harboring the R1078W mutation, in line with our hypothesis of an intramolecular folding of TRIO that would be disrupted by mutations. By analyzing the conformational prediction of the whole spectrin domain with the GEFD1 in complex with RAC1, we realized that the 8 spectrin repeats form a ring around the GEFD1 domain, preventing RAC1 access to the GEFD1 (Fig. 3B, RAC1 in turquoise). We therefore hypothesized that, when the interaction between DH1 and the 7th spectrin repeat is disrupted by mutations, this would lead to unfolding of the whole spectrin domain ring, allowing for better access of DH1 to the GTPase. We reasoned that, when introduced in the isolated GEFD1 domain alone, the activating mutations would bind and activate RAC1 like WT TRIO does, without hyperactivation. To address this point, we tested the ability of the D1368V, H1371Y and G1448R mutations in the isolated GEFD1 domain to bind and activate RAC1. We had shown previously that TRIO variants at the interface with RAC1 did not bind RAC^{N17} and were therefore defective in RAC1 activation [25]. As predicted, all three variants D1368V, H1371Y and G1448R bound RAC^{N17} as WT GEFD1 did (Fig. 3C, D), while the same variants in the context of the full-length protein showed increased RAC^{N17} binding in comparison with WT TRIO (Fig. 3E, F). Consistent with this result, all three variants in the GEDF1 context activated RAC1 only to wild-type levels (Fig. 3G, H). This result confirmed that the effect of these variants in the full-length TRIO protein (Fig. 1C) was dependent on the spectrin domain and could be due to disruption of the binding between DH1 and spectrin 7.

Based on these data, we propose a model wherein pathogenic variants targeting either the 7th spectrin domain or the DH1 residues relieve the autoinhibition of TRIO by disrupting the DH1-spectrin interaction, leading to the unfolding of the whole spectrin ring, which in turn allows full access to the GTPase. This model proposes an explanation as to how the pathogenic TRIO variants lead to RAC1 hyperactivation (Fig. 3I).

TRIO variants with opposite effect on RAC1 activation differentially impact TRIO-induced neurite development in vitro

TRIO is a well-established regulator of axon outgrowth and guidance via RAC1 activation, yet the impact of pathogenic TRIO variants on these neurodevelopmental processes is still unknown. To explore this, we investigated whether expression of pathogenic variants in cultured primary neurons affected neurite outgrowth, a process positively regulated by RAC1 [34]. We focused our study on two mutants from cluster 1 (TRIO-R1078W and -R1078Q) known to over-activate RAC1, and compared their effects to those of two mutants from cluster 2 (TRIO-E1299K and -R1428Q), which are defective in RAC1 activation [25]. The different GFP-tagged TRIO constructs were transfected into primary hippocampal neurons at DIV1 (Days in Vitro), and neurite length was measured at DIV3 (Fig. 4). As described earlier, the expression of TRIO-WT promoted RAC1-dependent neurite outgrowth [35]. Expression of both TRIO-E1299K and TRIO-R1428Q (cluster 2 variants) resulted in reduction of neurite outgrowth, which was expected, given that these variants are defective in RAC1 activation. Surprisingly, we found that TRIO variants R1078W/Q also led to reduced axon outgrowth, although they over-activate RAC1. By monitoring the presence of F-actin cytoskeleton structures in the neurons, using phalloidin staining, we noticed along the neurites of the TRIO-R1078W/Q-expressing neurons the presence of numerous lamellipodia, which were almost absent in neurons expressing TRIO-WT or TRIO variants R1428Q/E1299K (Fig. 4B, D). The presence of these aberrant lamellipodia in neurites was consistent with the enhanced RAC1 activation promoted by these variants, as RAC1 is known to promote the formation of these specific F-actin structures [25].

Interestingly, we also observed that only neurons expressing cluster 2 variants presented an increase in neurite branching (Fig. 4C, D). Of note, cluster 1 and 2 variants did not have any impact on the formation of neurites emerging from the soma, as the number of total neurites was not different between control neurons and neurons expressing the TRIO variants R1078W/Q or R1428Q/E1299K (Supplementary Fig. 2A).

Table 1. Individual clinical phenotypes.

Patient	**1**	**2**	**3**	**4**	**5**	**6**	**7**	**8**
Trio variant								
Coding change	c.3211C>G	c.3220T>C	c.3224C>T	c.3229G>C	c.3232C>T	c.3232C>T	c.3232C>T	c.3232C>T
Protein change	**p.Leu1071Val**	**p.Cys1074Arg**	**p.Thr1075Ile**	**p.Ala1077Pro**	**p.Arg1078Trp**	**p.Arg1078Trp**	**p.Arg1078Trp**	**p.Arg1078Trp**
Domain	Spectrin	Spectrin	Spectrin	Spectrin	Spectrin	Spectrin	Spectrin	Spectrin
Inheritance	De novo	De novo	De novo	De novo	De novo	De novo		De novo
Sex	M	M	F	F	F	F	F	M
Age last assessment	3 years	21 months	9 years	8 years	22 months	14 years	31 months	5 years
Development	Severe delay No speech	Global delay	Severe ID No speech	Severe ID	Severe ID	Moderate Global delay	Severe global delay Severe speech delay	Severe global delay Severe speech delay
Cranial dysmorphism	Relative macrocephaly OFC 50th, but height/weight <0,4th	Macrocephaly Broad forehead Reduced weight	Macrocephaly Growth retardation	Macrocephaly	Macrocephaly	High forehead High frontal hairline	Macrocephaly Prominent forehead	Macrocephaly
Seizures	–	Yes		Yes		Yes		Yes
Other NDDs					Poor attention	ADHD, ASD	Poor attention	
Other genetic variants	COL1A1 pathogenic variant		Homozyg. GMPPA variant c.1169G>A			DYNC1H1-VUS		
Other findings	Osteogenesis imperfecta	Severe axial limb hypotonia Agenesis of corpus callos.	Muscular hypotonia, Stereotypic movements			MRI PVL-PVNH	Moderate hypotonia Arnold-Chiari malformation	Neuropathic bladder Intestinal malrotation
Patient ref.	This study	24	24	This study	This study	This study	This study	This study
Variant described in	–	24	24, 25	–	25	25	25	25
Patient	**9**	**10**	**11**	**12**	**13**	**14**		
Trio variant								
Coding change	c.3371T>C	c.3421G>A	c.3475G>A	c.4103A>T	c.4111C>T	c.4342G>A		
Protein change	**p.Leu1124Ser**	**p.Val1141Met**	**p.Glu1159Lys**	**p.Asp1368Val**	**p.His1371Tyr**	**p.Gly1448Arg**		
Domain	Spectrin	Spectrin	Spectrin	GEFD1	GEFD1	GEFD1		
Inheritance		De novo	De novo	De novo	De novo			
Sex	F	F	F	M	M	M		
Age last assessment	20 years	11 years	8 yrs 7 months	27 months		7 years		
Development	Moderate ID	Severe ID	Global delay	Severe ID Few words	Severe ID Absent speech	Severe ID		
Cranial dysmorphism			Frontal bossing, short palpebral fissures	Relative macrocephaly Short stature Downslanting palpebr. fissures	Macrocephaly	Macrocephaly		

Table 1. continued

Seizures	Mild myoclonus				Yes	
Other NDDs		Hyperactivity ASD	Agression ADHD, ASD			
Other genetic variants		Pathogenic variant in intron 16 of FOXP1 c.1428 + 1G>C		Variant in PDHA1	Dup 12q24.32 paternally inherited	
Other findings	Dystonia	Motor and language disorder	Muscular hypotonia	Mild dilation of ventricules	Agressive behavior	Insensitivity to pain
Patient	This study	This study	This study	23	32	This study
Variant described in	–	–	–	20, 23	32	–

Description of the clinical phenotype observed among TRIO mutation carriers, grouped on the basis of variant location or protein effect: spectrin repeat and GEFD1.
ADHD attention deficit hyperactivity disorder, *ASD* autism spectrum disorder, *M* male; *F* female, *ID* intellectual disability, *NDD* neurodevelopmental disorder, *PVL* periventricular leukomalacia, *PVNH* periventricular nodular heterotopia.

Combined, our data show that the TRIO variants of clusters 1 and 2, which affect RAC1 activation in opposite ways, differentially impact on neuronal morphology. The expression of TRIO variants of cluster 1 impairs neurite outgrowth probably by an excessive induction of F-actin-based lamellipodia along the neurite, thus preventing normal neurite outgrowth. In contrast, expression of cluster 2 variants induces neurite branching, and slightly reduces neurite outgrowth, most likely due to their deficiency in promoting adequate F-actin remodeling because of impaired RAC1 activation.

TRIO variants of clusters 1 and 2 differentially affect growth cone morphology and dynamics

Axon outgrowth and guidance is driven by the growth cone at the tip of the axon, which integrates the signals of extracellular guidance cues and translates them into signaling pathways leading to cytoskeletal remodeling, which in turn promotes shape changes and movement [3]. Given the importance of RAC1 activity in growth cone dynamics, we analyzed the morphology and the dynamics of the growth cones following expression of the TRIO variants in primary neurons. The growth cone perimeter of the TRIO-R1078W-expressing hippocampal neurons, and to a lesser extent that of TRIO-R1078Q-expressing cells, increased dramatically compared to TRIO-WT-expressing growth cones. In contrast, the expression of cluster 2 variants led to a reduction of the growth cone size (Fig. 5A–C). In addition, we noticed that the number of filopodia increased in the TRIO-R1078W and TRIO-R1078Q expressing growth cones (Supplementary Fig. 2B). However, given that the number of filopodia is strictly correlated to the size of the growth cone, we found that the number of filopodia relative to the growth cone surface was unchanged in the different conditions (Supplementary Fig. 2C).

We subsequently monitored the effect of TRIO variants on filopodia dynamics, by performing live-imaging microscopy on axonal growth cones of neurons co-expressing GFP-TRIO variants and the F-actin reporter Lifeact-Tq (Fig. 5D, E). The expression of TRIO-WT led to an increase in the number of both filopodia extensions and retractions, which is consistent with a normal RAC1 activation. In contrast, neurons expressing cluster 2 variants presented a strong reduction in the number of both filopodia extensions and retractions, which reflects a reduced F-actin turnover due to deficient RAC1 activation. Interestingly, while we observed a strong increase in the number of filopodia extensions following expression of TRIO variants of cluster 1 as compared to TRIO-WT, we observed no change in the number of retractions, suggesting that TRIO-R1078W/Q overexpression triggers a robust elongation or stabilization of F-actin bundles in filopodia. Based on these data, we conclude that TRIO variants of clusters 1 and 2 affect F-actin turnover in different ways, leading to distinct defects in growth cone morphology and dynamics.

TRIO variants of cluster 1 and 2 differentially affect TRIO-regulated axon development in vivo

We investigated whether the expression of these TRIO variants impacted neuronal development in vivo, in the zebrafish *Danio Rerio*. To this end, we chose to focus on the zebrafish motor system, based on the following rationale: (i) TRIO plays an essential role in motoneuron axon outgrowth and pathfinding in invertebrate models, through RAC1 activation [14, 36]; (ii) zebrafish spinal motor neuron (SMN) projections have been well characterized and develop in a highly stereotyped manner, making the detection of connectivity defects relatively easy (Fig. 6A); (iii) finally, we have successfully used an equivalent strategy to characterize the pathogenic impact of glycine receptor variants found in patients with ASD [37].

To analyze the impact of key TRIO mutations identified in cluster 1 and 2 on spinal motor neuron morphology at a single neuron scale in vivo, we used the UAS/GAL4 system to conduct

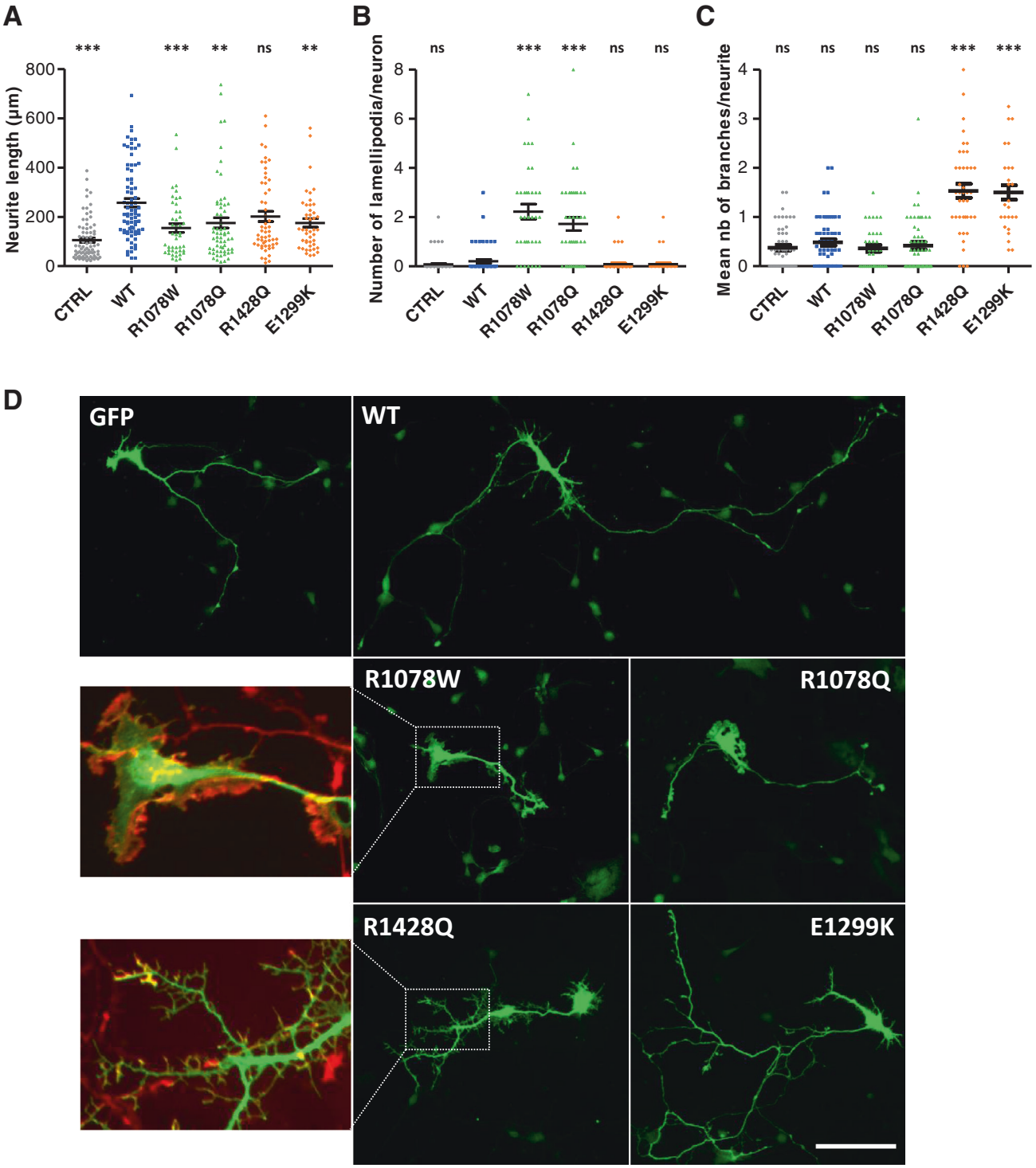

Fig. 4 TRIO variants of clusters 1 and 2 differentially affect neuronal morphology. Quantification of neurite length (**A**), number of lamellipodia per neuron (**B**) and number of branches per neurite (**C**) in TRIO-variant-expressing neurons as indicated. **D** Representative micrographs of immunostained DIV3 hippocampal neurons overexpressing the different GFP-TRIO constructs. Phalloidin TRITC staining (red) reveals lamellipodia formation occurring in TRIO R1078Q/W overexpressing neurons (inset on the left). Neurons expressing TRIO R1428Q and E1299K variants show an increased number of branches (inset on the left). Quantification was made from 4 independent experiments. Scale bar: 100 µm. **A**–**C** $^{**}p \leq 0.01$; $^{***}p \leq 0.001$; one-way ANOVA, Dunnett test.

transient transgenesis experiments. To this aim, human WT and mutated TRIO cDNAs were cloned under a 14UAS promoter and fused via a T2A cleavable peptide to a membrane-targeted GFP, a strategy allowing the visualization of the whole morphology of TRIO-expressing neurons. These constructs were then injected in the Tg(HuC:GAL4) driver line to drive mosaic expression of TRIO variants in spinal motor neurons. The impact of TRIO WT and pathogenic variants on SMN axon outgrowth and pathfinding was analyzed in 72-hpf transgenic larvae immunolabeled with GFP and Zn-5 antibodies to label TRIO-expressing versus non-expressing

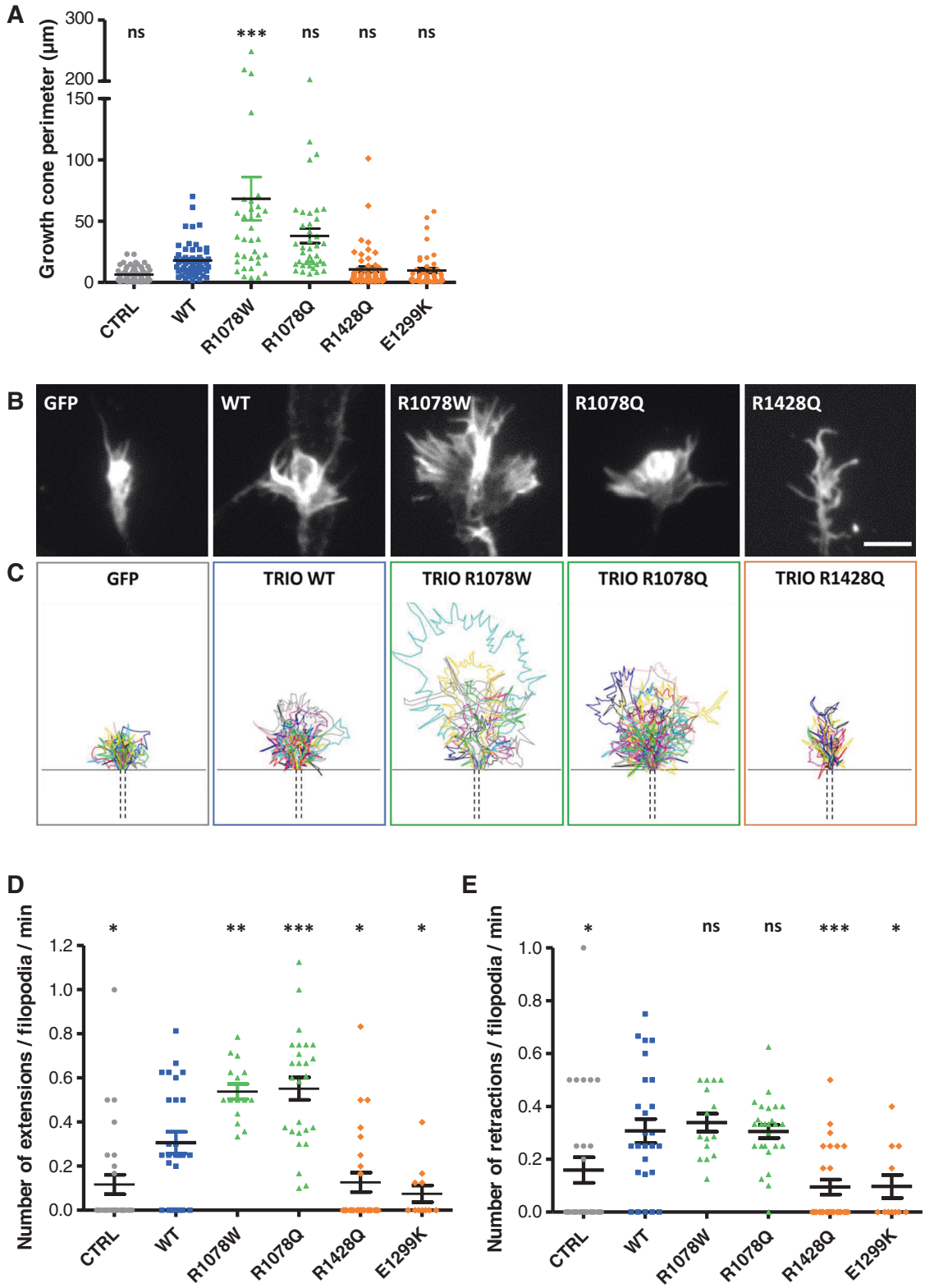

Fig. 5 TRIO variants affect growth cone morphology and alter F-actin dynamics. A Measurement of the growth cone perimeter in immunostained DIV3 neurons expressing TRIO variants as indicated, from 5 independent experiments. **B** Representative micrographs of the growth cone morphology of DIV3 neuronal growth cones expressing TRIO variants. **C** Plotted ROIs representing the shape of GFP ($n = 54$), TRIO-WT ($n = 24$), TRIO-R1078W ($n = 13$), TRIO-R1078Q ($n = 32$) or TRIO-R1428Q ($n = 15$) expressing growth cones and generated by the "Growth cone visualiser" ImageJ macro. **D, E** Quantification of filopodia dynamics using live-imaging on TRIO-variants-expressing growth cones. Number of **(D)** extensions and **(E)** retractions per filopodia per minute, from 5 independent experiments. Neurons used for **(A)** and **(D, E)** quantifications were the same. The growth cone perimeter has been calculated before the start of the movie. Scale bar: 10 µm. **A, D, E** $*p \leq 0.05$; $**p \leq 0.01$; $***p \leq 0.001$; one-way ANOVA, Dunnett test.

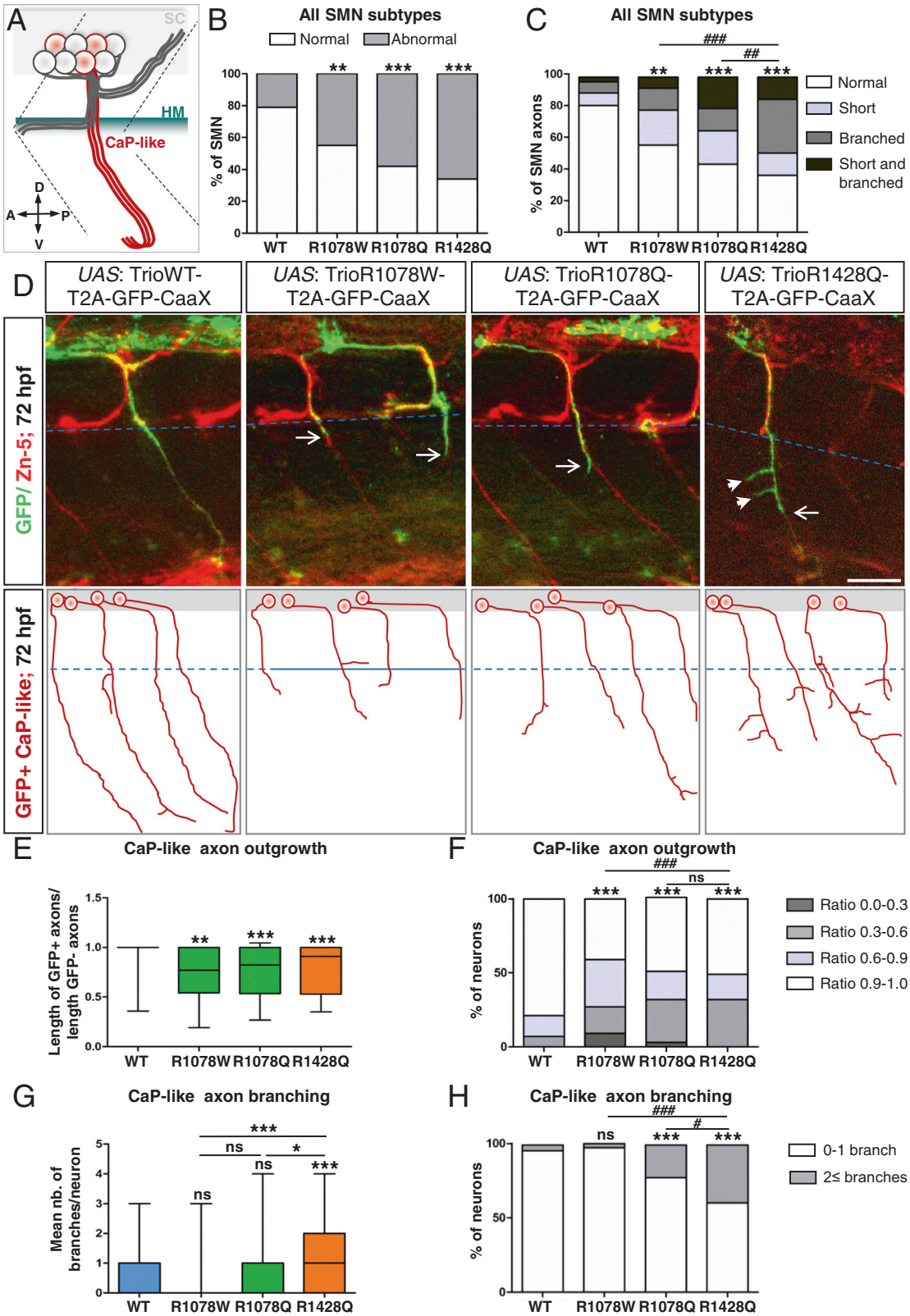

SMNs, respectively. While 80% of TRIO-WT-GFP expressing SMNs developed normally compared to GFP-negative SMNs, this number was decreased to 55% and 40% for SMNs expressing TRIO-R1078W and TRIO-R1078Q, respectively. The percentage of motor neurons showing normal axon targeting was even more reduced for the cluster 2 TRIO-R1428Q variant (Fig. 6B). By looking more carefully at their morphology, we noticed that cluster 1 expressing SMNs mainly displayed shorter axons as compared to TRIO WT-expressing SMNs, while R1428Q-expressing neurons exhibited both short and hyperbranched axons (Fig. 6C). To refine

Fig. 6 TRIO variants of cluster 1 and 2 differentially affect axonal development in the zebrafish. A Schematic representation of the stereotypic organization of spinal motor neuron (SMN) projections in the zebrafish larvae. Ventrally projecting motor neurons (CaP) are highlighted in red, while rostrally and dorsally projecting motor neurons are indicated in gray. Light gray and blue regions indicate the spinal cord (SC) and the horizontal myoseptum (i.e. key guidance choice point; HM), respectively. **B**–**H** Neuronal-targeted expression of wild type (WT), spectrin (R1078W, R1078Q) or GEFD1 (R1428Q) TRIO variants together with a membrane GFP (GFP-CAAX) in zebrafish larvae using the *UAS/GAL4* system. The membrane-targeted GFP was used to visualize the whole morphology of human TRIO-expressing motor neurons. **B** Percentage of GFP+ motor neurons with abnormal morphology. **C** Distribution of the morphological defects associated with the overexpression of the different TRIO constructs. **B, C** A total of 219 WT, 55 R1078W, 156 R1078Q and 118 R1428Q positive SMNs were included in these quantifications. **D** Upper panels: Immunolabelling of SMN in 72-hpf Tg(*HuC*:GAL4) transgenic larvae injected with *UAS*:TRIOWT-T2A-GFP-CAAX, *UAS*:TRIOR1078W-T2A-GFP-CAAX, *UAS*:TRIOR1078Q-T2A-GFP-CAAX or *UAS*:TRIOR1428Q-T2A-GFP-CAAX construct using Zn-5 and GFP antibodies. Lateral views of the trunk with a special focus on ventrally-projecting axons (CaP-like); anterior to the left. Blue dotted lines delineate the horizontal myoseptum. Arrows indicate shorter CaP-like axons. Arrowheads point at ectopic branches. Scale bar: 25µm. Lower panels: Representative schematics of the morphology of GFP + CaP-like axons overexpressing human WT TRIO or pathogenic variants. **E** Quantification of the mean axonal length ratio of GFP + CaP-like axons normalized to GFP- CaP-like axons, for each TRIO construct. **F** Distribution of neuronal length in each category calculated from result presented in (**E**), for each TRIO constructs. **G** Mean number of branches per GFP+ CaP-like axons. **H** Distribution of CaP-like neurons according to their number of branches for each TRIO constructs. **E**–**H** Quantifications were carried out on 71 TRIO-WT, 34 TRIO-R1078W, 113 TRIO-R1078Q and 63 TRIO-R1078W CaP-like neurons observed in 29, 15, 23 and 30 transgenic embryos respectively. (**B**, **C**, **F**, **H**) Chi-square test (χ^2 test) was used to statistically compare the distribution of the motor neuron phenotypes observed in zebrafish larvae expressing the different TRIO constructs. *$p \leq 0.05$; **$p \leq 0.01$; ***$p \leq 0.001$ for TRIO-WT versus TRIO-variants; $^{\#}p \leq 0.05$; $^{\#\#}p \leq 0.01$; $^{\#\#\#}p \leq 0.001$ for TRIO variant from Cluster 1 versus Cluster 2; χ^2 test. **E**, **G** Box and Whisker graphs. *$p \leq 0.05$; ***$p \leq 0.001$; ns non-significant; Kruskal–Wallis ANOVA test with Dunn's post-test. Whiskers indicate the Min/Max values.

our characterization of the impact of human TRIO variants on SMN axon outgrowth and targeting, we focused our analysis on one SMN subtype, the CaP-like neurons, whose low-complexity, ventrally-projecting axons are easy to track (Fig. 6A, D). Axon outgrowth of CaP-like neurons was significantly impaired following expression of variants of both clusters, with the TRIO-R1078W-expressing neurons presenting the shortest axons (Fig. 6D–F). In contrast, expression of TRIO-R1428Q in CaP-like neurons significantly increased the number of axon branches, compared to TRIO-R1078W, TRIO-R1078Q and TRIO-WT expression (Fig. 6D, G). Notably, about 40% of the TRIO-R1428Q-expressing CaP-like neurons exhibited more than two supernumerary branches, compared to TRIO-R1078W (3%), TRIO-R1078Q (22%) and TRIO-WT (4%) expressing neurons (Fig. 6D, H).

Altogether, these data show that TRIO variants of both clusters, which have opposite effects on RAC1 activity, differentially affect axon outgrowth/targeting in vivo in a vertebrate model. Interestingly, the axonal defects associated with pathogenic TRIO variant expression in the zebrafish SMNs strikingly mimic those described in murine hippocampal neurons. This study therefore provides the first in vivo evidence of the impact of pathogenic TRIO gain- and loss-of-function variants on vertebrate neuronal development and strengthens their potential contribution to the disruption of neuronal connectivity in the brain of affected individuals.

DISCUSSION

NDDs are complex disorders with large genetic components, but despite intensive efforts, our understanding of the contribution of monogenic mutations in the etiology of the diseases remains elusive. We have previously identified a number of variants in the *TRIO* gene that all fall into cluster 1 and cause RAC1 hyperactivation. These mutations are of particular interest as they are gain-of-function mutations associated with severe developmental delay, and are the most recurrent variants found in individuals with TRIO disorders [25].

TRIO disorders belong to the expanding family of RAC-related neurodevelopmental diseases [38] that have attracted a growing interest, due to the central role of RAC signaling pathways in brain development. They include pathogenic variations in the *RAC1* and *RAC3* genes themselves, but also in genes encoding either RAC effectors such as PAK1 and PAK3, or more recently regulators of RAC such as TRIO [38]. Similar to TRIO, activating gain-of-function mutations have been also identified in PAK1 and are associated with severe neurodevelopmental delay [39, 40]. These findings suggest that gain-of-function mutations associated to RAC1 overactivation represent a general pathogenic mechanism shared by this group of RAC-related neurodevelopmental disorders. They also reinforce the needs to investigate how these novel gain-of-function mutations disrupt the control of TRIO activity, and how they impact on neuronal development.

New molecular insights on how TRIO activating mutations perturb the regulation of TRIO activity came from our analysis of new TRIO variants associated with neurodevelopmental disorders. Indeed, we report here an important number of new variants leading to RAC hyperactivation and associated with severe ID. Some of these *de novo* variations target previously identified recurrent mutations of cluster 1, as expected, but we also identified new amino acids in the same spectrin α-helix targeted by mutations (5 amino acids in total, from 1071 to 1078). Combined with our previous study, it is noteworthy that so far, 17 unrelated individuals with variants in cluster 1 have been identified. Most of the patients carrying these variants present with macrocephaly, reinforcing the phenotype/genotype correlation we had made previously [25] and confirming the contribution of cluster 1 variants to the pathogenicity of severe TRIO-associated NDDs. Surprisingly, among the RAC1-activating mutations associated to macrocephaly in patients, we also found mutations in GEFD1. It should be noted that most of the previously reported mutations in GEFD1 had been shown to impair RAC activation and to be associated to microcephaly [22, 23, 25]. In our study, the in-depth analysis of these activating NDD-associated TRIO variants has served unraveling and proposing a novel mechanism for the autoinhibition of TRIO activity, which would be released by pathogenic mutations. Indeed, the molecular mechanism by which TRIO variants from cluster 1 lead to RAC1 overactivation was intriguing, since the spectrin repeats had no catalytic activity towards RAC1 per se. We show here that the TRIO GEF activity is required for TRIO-R1078W variant induced overactivation of RAC1. This result excludes the possibility that the TRIO-R1078W variant promotes the recruitment and activation of another RAC1 regulator that would lead to RAC1 overactivation. This suggests that TRIO-R1078W over-activates RAC1 via the disruption of TRIO folding, which in turn may facilitate the access to RAC1.

Combined, the data presented here allow us to propose a working model that would explain how the different mutations identified in patients with severe condition could lead to hyperactivation of RAC1 (Fig. 3I). We propose that under physiological conditions, there is a tightly controlled regulation of TRIO GEF activity by the spectrin repeats that form a ring surrounding the GEFD1. This molecular interaction between the 7th spectrin domain and GEFD1 would prevent the latter from binding and activating RAC1. This is mediated by the 7th spectrin domain with R1078 playing a dual central role. On one hand,

R1078 is engaged in the stabilization of the 7th spectrin repeat, most probably by making a strong electrostatic interaction with E1120 in the adjacent α-helix of the repeat. On the other hand, R1078 is in close proximity to and most likely interacts with residues in DH1. Further experiments are required to validate this specific interaction. Importantly, the fact that R1078 plays such a crucial role in the control of TRIO folding is consistent with the observation that this amino acid is the most recurrently targeted by mutation in TRIO patients.

When these residues are mutated in pathological conditions, whether in the spectrin stretch or in the DH1 residues, the folding of the spectrin ring structure would be released, allowing for better access of DH1 to RAC1, and thus leading to uncontrolled hyperactivation of RAC1 (Fig. 3I). This is consistent with the similar phenotype observed in patients with these specific variants in the two domains. Interestingly, this model also allows us to propose an explanation as to why mutations in residues D1368, H1371 and G1448 do not lead to RAC1 inactivation, but rather to RAC1 overactivation in the context of the full-length protein. Indeed, these residues are not at the interface with the RAC1 GTPase, unlike the RAC-hypo-activating variants described earlier [25]. Consistent with this observation, mutations of these residues do not affect RAC1 binding and activation in the context of the isolated GEFD1 domain. Combined, these results confirm that the activating effect of these variants in the full-length protein is dependent on the spectrin domains. Whether this is due to intramolecular interactions or oligomerization of TRIO moieties remains to be established in future studies. In conclusion, our work provides a molecular explanation on how TRIO activity may be inhibited by complex molecular folding involving the whole spectrin repeat domain and the GEFD1, and how this folding would be disrupted by pathogenic mutations. Interestingly, a similar model of TRIO GEFD1 autoinhibition by the spectrin domains has been shown by recent work by Koleske et al, and published during the reviewing process of our work [41]. Indeed, using different in vitro assays complementary to ours, they showed that the spectrin repeats make complex contacts with the GEFD1, thus inhibiting GEFD1 activity towards RAC1, and that disorder-associated variants are sufficient to relieve this auto-inhibitory constraint. In addition, it has been recently shown that introducing the previously described N1080I in the context of the D1368V variant abrogates RAC1 overactivation by D1368V, suggesting that the N1080 participates to another mode of regulation of TRIO GEF activity than the one we describe here [42]. This suggests that the regulation of TRIO activity is complex and needs further investigation.

Axon outgrowth and guidance is a complex neurodevelopmental process required for the establishment of correct neuronal connectivity. In this study, we show that pathogenic gain-of-function and loss-of-function TRIO variants induce different defects in axon outgrowth and branching both in vitro and in vivo, in the zebrafish model. The axonal defects of zebrafish motoneurons expressing pathogenic TRIO variants phenocopy those observed in cultured murine hippocampal neurons transfected with TRIO variants. Our work provides the first evidence of the impact of TRIO variants in a whole organism and emphasizes the relevance and robustness of the zebrafish model for characterizing the pathogenic impact of novel genetic variants in NDDs.

TRIO variants from cluster 1 impair axonal outgrowth, both in vitro when expressed in hippocampal neurons and in vivo when expressed in zebrafish motor neurons. This is consistent with the observation made in a KO mouse model of ARHGAP15, a negative regulator of RAC1, which represents an in vivo model of RAC hyperactivation [43]. Cortical neurons from these mice display several defects, including shorter axons in vitro and in vivo. Axon outgrowth and guidance processes are driven by the highly dynamic growth cone at the tip of the axon that undergoes F-actin cytoskeleton remodeling to promote shape changes and motility in response to extracellular guidance cues. Our results show that hyperactivation of RAC1 by the gain-of-function mutations induces an increase in growth cone size. Moreover, the filopodia extension rate is increased, while the retraction rate does not change as compared to TRIO-WT, probably generating stable filopodia-rich protrusions. Based on our data, we propose a model whereby axon outgrowth is impaired by an excessive F-actin remodeling in the growth cone, induced by an over-activation of RAC1 by TRIO gain-of-function mutations. Furthermore, the ectopic lamellipodia formation associated with these variants could represent a physical barrier preventing microtubule growth in the growth cone. Indeed, in addition to F-actin remodeling, the presence of exploratory MTs in the growth cone is essential to sustain axon outgrowth and control axon pathfinding [44]. Further experiments are needed to explore this hypothesis.

Several molecular mechanisms could explain how TRIO variants from cluster 1 induce an increase in filopodia extension inside the growth cone. Overactivation of RAC1 could lead to an increase in polymerization or a decrease in depolymerization of actin filaments by acting on the different actin-regulating proteins playing a central role in filopodia formation [45]. An alternative mechanism could be that TRIO via RAC1 negatively controls the actin retrograde flow, which is induced by the pushing forces against the plasma membrane generated by actin polymerization [46]. Future work should examine the contribution of these different hypotheses to the effect of pathogenic TRIO variants of cluster 1 on F-actin remodeling.

Cluster 2 variants are impaired in axon outgrowth, most probably because they are defective in RAC1 activation. Axons are shorter both in hippocampal neurons and in zebrafish motor neurons. The hypoactivation of RAC1 by cluster 2 variants reduces the size of the growth cone, which presents mostly static filopodia. Interestingly, the most striking phenotype is the presence on the axons of numerous branches both in vitro and in vivo, in zebrafish motor neurons. RAC proteins are known to control multiple aspects of axonal development in different systems from invertebrates to mammals including axon branching [47]. However, contradictory findings have been published concerning the effect of RAC1 overactivation or inhibition in different systems [34]. In line with our findings, *C. elegans* carrying mutations in *RAC* and *unc-73* (TRIO ortholog) also display defects in axonal development, including the formation of ectopic axon branches [48, 49]. From these results, we can propose that vertebrate TRIO, like UNC-73 and RAC proteins in *C. elegans*, restricts the number of branches through RAC1 activation, and that TRIO mutants from cluster 2, which are defective in RAC1 activation, are not able to do so. Whether these ectopic branches are still able to make productive synaptic contacts remains to be determined.

In summary, by combining clinical, molecular, cellular and in vivo data, we provide new evidence for the pathogenicity of novel genetic variants targeting TRIO in NDDs. Our data demonstrate that pathogenic TRIO mutations have a strong impact on neuronal development in vivo. In addition, we propose a novel mechanism whereby the auto-inhibited state of TRIO, likely due to intramolecular folding, is disrupted by pathogenic mutations in TRIO, which may lead to the perturbation of neuronal connectivity in the brain of individuals suffering from these emerging disorders.

REFERENCES

1. Vissers LELM, Gilissen C, Veltman JA. Genetic studies in intellectual disability and related disorders. Nat Rev Genet. 2016;17:9–18.
2. Gomez TM, Letourneau PC. Actin dynamics in growth cone motility and navigation. J Neurochem. 2014;129:221–34.

3. Dent EW, Gupton SL, Gertler FB. The growth cone cytoskeleton in axon outgrowth and guidance. Cold Spring Harb Perspect Biol. 2011;3:a001800.
4. Govek EE, Newey SE, Van Aelst L. The role of the Rho GTPases in neuronal development. Genes Dev. 2005;19:1–49.
5. Schmidt S, Debant A. Function and regulation of the Rho guanine nucleotide exchange factor Trio. Small GTPases. 2014;5:e29769.
6. Bircher JE, Koleske AJ. Trio family proteins as regulators of cell migration and morphogenesis in development and disease - mechanisms and cellular contexts. J Cell Sci. 2021;134:jcs248393.
7. Paskus JD, Herring BE, Roche KW. Kalirin and trio: RhoGEFs in synaptic transmission, plasticity, and complex brain disorders. Trends Neurosci. 2020;43:505–18.
8. O'Brien SP, Seipel K, Medley QG, Bronson R, Segal R, Streuli M. Skeletal muscle deformity and neuronal disorder in trio exchange factor-deficient mouse embryos [In Process Citation]. Proc Natl Acad Sci USA. 2000;97:12074–8.
9. Zong W, Liu S, Wang X, Zhang J, Zhang T, Liu Z, et al. Trio gene is required for mouse learning ability. Brain Res. 2015;1608:82–90.
10. Katrancha SM, Shaw JE, Zhao AY, Myers SA, Cocco AR, Jeng AT, et al. Trio haploinsufficiency causes neurodevelopmental disease-associated deficits. Cell Rep. 2019;26:2805–17.e9.
11. Debant A, Serra-Pages C, Seipel K, O'Brien S, Tang M, Park SH, et al. The multidomain protein Trio binds the LAR transmembrane tyrosine phosphatase, contains a protein kinase domain, and has separate rac- specific and rho-specific guanine nucleotide exchange factor domains. Proc Natl Acad Sci USA 1996;93:5466–71.
12. Chhatriwala MK, Betts L, Worthylake DK, Sondek J. The DH and PH domains of Trio coordinately engage Rho GTPases for their efficient activation. J Mol Biol. 2007;368:1307–20.
13. Bellanger JM, Estrach S, Schmidt S, Briancon-Marjollet A, Zugasti O, Fromont S, et al. Different regulation of the Trio Dbl-Homology domains by their associated PH domains. Biol Cell. 2003;95:625–34.
14. Chen SY, Huang PH, Cheng HJ. Disrupted-in-Schizophrenia 1-mediated axon guidance involves TRIO-RAC-PAK small GTPase pathway signaling. Proc Natl Acad Sci USA 2011;108:5861–6.
15. Neubrand VE, Thomas C, Schmidt S, Debant A, Schiavo G. Kidins220/ARMS regulates Rac1-dependent neurite outgrowth by direct interaction with the RhoGEF Trio. J Cell Sci. 2010;123:2111–23.
16. van Haren J, Boudeau J, Schmidt S, Basu S, Liu Z, Lammers D, et al. Dynamic microtubules catalyze formation of navigator-TRIO complexes to regulate neurite extension. Curr Biol. 2014;24:1778–85.
17. Sanders SJ, Murtha MT, Gupta AR, Murdoch JD, Raubeson MJ, Willsey AJ, et al. De novo mutations revealed by whole-exome sequencing are strongly associated with autism. Nature. 2012;485:237–41.
18. O'Roak BJ, Vives L, Girirajan S, Karakoc E, Krumm N, Coe BP, et al. Sporadic autism exomes reveal a highly interconnected protein network of de novo mutations. Nature. 2012;485:246–50.
19. Iossifov I, O'Roak BJ, Sanders SJ, Ronemus M, Krumm N, Levy D, et al. The contribution of de novo coding mutations to autism spectrum disorder. Nature. 2014;515:216–21.
20. de Ligt J, Willemsen MH, van Bon BWM, Kleefstra T, Yntema HG, Kroes T, et al. Diagnostic exome sequencing in persons with severe intellectual disability. N Engl J Med. 2012;367:1921–9.
21. Ba W, Yan Y, Reijnders MRF, Schuurs-Hoeijmakers JHM, Feenstra I, Bongers EMHF, et al. TRIO loss of function is associated with mild intellectual disability and affects dendritic branching and synapse function. Hum Mol Genet. 2016;25:892–902.
22. Pengelly R, Greville-Heygate S, Schmidt S, Seaby E, Fagotto-Kaufmann C, Jabalameli R, et al. Mutations specific to the Rac-GEF domain of TRIO cause intellectual disability and microcephaly. J Med Genet. 2016;53:735–42.
23. Sadybekov A, Tian C, Arnesano C, Katritch V, Herring BE. An autism spectrum disorder-related de novo mutation hotspot discovered in the GEF1 domain of Trio. - PubMed - NCBI. Nat Comm. 2017;8:601.
24. Kloth K, Graul-Neumann L, Hermann K, Johannsen J, Bierhals T, Kortüm F. More evidence on TRIO missense mutations in the spectrin repeat domain causing severe developmental delay and recognizable facial dysmorphism with macrocephaly. Neurogenetics. 2021;22:221–4.
25. Barbosa S, Greville-Heygate S, Bonnet M, Godwin A, Fagotto-Kaufmann C, Kajava AV, et al. Opposite modulation of RAC1 by mutations in TRIO is associated with distinct, domain specific neurodevelopmental disorders. Am J Hum Genet. 2020;106:338–55.
26. Jumper J, Evans R, Pritzel A, Green T, Figurnov M, Ronneberger O, et al. Highly accurate protein structure prediction with AlphaFold. Nature. 2021;596:583–9.
27. Cannet A, Schmidt S, Delaval B, Debant A. Identification of a mitotic Rac-GEF, Trio, that counteracts MgcRacGAP function during cytokinesis. Mol Biol Cell. 2014;25:4063–71.
28. Akerboom J, Chen T-W, Wardill TJ, Tian L, Marvin JS, Mutlu S, et al. Optimization of a GCaMP Calcium Indicator for Neural Activity Imaging. J Neurosci. 2012;32:13819–40.
29. Kimmel CB, Ballard WW, Kimmel SR, Ullmann B, Schilling TF. Stages of embryonic development of the zebrafish. Dev Dynt. 1995;203:253–310.
30. Horstick EJ, Jordan DC, Bergeron SA, Tabor KM, Serpe M, Feldman B, et al. Increased functional protein expression using nucleotide sequence features enriched in highly expressed genes in zebrafish. Nucleic Acids Res. 2015;43:e48.
31. Raynaud F, Janossy A, Dahl J, Bertaso F, Perroy J, Varrault A, et al. Shank3-Rich2 interaction regulates AMPA receptor recycling and synaptic long-term potentiation. J Neurosci. 2013;33:9699–715.
32. Aspromonte MC, Bellini M, Gasparini A, Carraro M, Bettella E, Polli R, et al. Characterization of intellectual disability and autism comorbidity through gene panel sequencing. Hum Mutat. 2019;40:1346–63.
33. Katrancha SM, Wu Y, Zhu M, Eipper BA, Koleske AJ, Mains RE. Neurodevelopmental disease-associated de novo mutations and rare sequence variants affect TRIO GDP/GTP exchange factor activity. Hum Mol Genet. 2017;26:4728–40.
34. Hall A, Lalli G. Rho and Ras GTPases in axon growth, guidance, and branching. Cold Spring Harb Perspect Biol. 2010;2:a001818.
35. Briancon-Marjollet A, Ghogha A, Nawabi H, Triki I, Auziol C, Fromont S, et al. Trio mediates netrin-1-induced Rac1 activation in axon outgrowth and guidance. Mol Cell Biol. 2008;28:2314–23.
36. Song JK, Giniger E. Noncanonical Notch function in motor axon guidance is mediated by Rac GTPase and the GEF1 domain of Trio. Dev Dyn. 2011;240:324–32.
37. Pilorge M, Fassier C, Le Corronc H, Potey A, Bai J, De Gois S, et al. Genetic and functional analyses demonstrate a role for abnormal glycinergic signaling in autism. Mol Psychiatry. 2016;21:936–45.
38. Scala M, Nishikawa M, Nagata K-I, Striano P. Pathophysiological mechanisms in neurodevelopmental disorders caused by Rac GTPases dysregulation: what's behind neuro-RACopathies. Cells. 2021;10:3395.
39. Harms FL, Kloth K, Bley A, Denecke J, Santer R, Lessel D, et al. Activating mutations in PAK1, encoding p21-activated kinase 1, cause a neurodevelopmental disorder. Am J Hum Genet. 2018;103:579–91.
40. Horn S, Au M, Basel-Salmon L, Bayrak-Toydemir P, Chapin A, Cohen L, et al. De novo variants in PAK1 lead to intellectual disability with macrocephaly and seizures. Brain J Neurol. 2019. https://doi.org/10.1093/brain/awz264.
41. Bircher J, Corcoran EE, Lam TT, Trnka MJ, Koleske AJ. Autoinhibition of the GEF activity of cytoskeletal regulatory protein Trio is disrupted in neurodevelopmental disorder-related genetic variants. J Biol Chem. 2022;298:102361.
42. Tian C, Jd P, E F, Kw R, Be H. Autism spectrum disorder/intellectual disability-associated mutations in trio disrupt neuroligin 1-mediated synaptogenesis. J Neurosci. 2021;41:7768–78.
43. Zamboni V, Armentano M, Berto G, Ciraolo E, Ghigo A, Garzotto D, et al. Hyperactivity of Rac1-GTPase pathway impairs neuritogenesis of cortical neurons by altering actin dynamics. Sci Rep. 2018;8:7254.
44. Dogterom M, Koenderink GH. Actin-microtubule crosstalk in cell biology. Nat Rev Mol Cell Biol. 2019;20:38–54.
45. Korobova F, Svitkina T. Arp2/3 complex is important for filopodia formation, growth cone motility, and neuritogenesis in neuronal cells. Mol Biol Cell. 2008;19:1561–74.
46. Minegishi T, Inagaki N. Forces to drive neuronal migration steps. Front Cell Dev Biol. 2020;0:863.
47. Lundquist EA. Rac proteins and the control of axon development. Curr Opin Neurobiol. 2003;13:384–90.
48. Struckhoff EC, Lundquist EA. The actin-binding protein UNC-115 is an effector of Rac signaling during axon pathfinding in *C. elegans*. Development. 2003;130:693–704.
49. Lundquist EA, Reddien PW, Hartwieg E, Horvitz HR, Bargmann CI. Three *C. elegans* Rac proteins and several alternative Rac regulators control axon guidance, cell migration and apoptotic cell phagocytosis. Development. 2001;128:4475–88.

ACKNOWLEDGEMENTS

We are grateful to all the patients and their families for their participation in this study, and in particular to Candice Williams. We also acknowledge Eva-Lena Stattin (Department of Immunology, Genetics and Pathology, Uppsala University, Uppsala, Sweden) and Philip Wyatt (Department of Obstetrics and Gynecology, York Central Hospital, Toronto, Ontario, Canada) for their patient case contribution.

We thank all members of the Debant team as well as Xavier Nicol (Institut de la Vision, Paris) for helpful discussions, and Damien Laouteouet and Jean-Christophe Perez for generating and performing initial experiments with the artificial spectrin mutants. This work was supported by grants from the Agence Nationale de la Recherche to AD (ANR-2019 TRIOTISM) and to CF (ANR-20-CE16-0019) and from The

Fondation pour la Recherche Médicale (program Equipes FRM2016, DEQ20160334942) to AD. MaxB and MarB are recipients of a PhD fellowship from the Ministère de l'Enseignement Supérieur et de la Recherche (MESR). DB is generously supported by a National Institute for Health and Care Research research professorship RP-2016-07-011. We acknowledge the imaging facility MRI, and in particular Volker Bäcker, part of the national France-BioImaging infrastructure supported by the French National Research Agency (ANR-10-INBS-04, "Investments for the future").

AUTHOR CONTRIBUTIONS

MaxB, AD, CF and SS conceived research and designed research experiments; DB, GG, DH, MPR, AC, DS, MM, FV and AC conducted subject recruitment and consented assessment; DB and GG interpreted subjects phenotypes; MaxB, CFK, IT, SS, FC and SB performed site-directed mutagenesis, cloning of plasmids, Western Blot and pulldown experiments; MaxB and SB prepared neuronal cultures; MaxB performed immunofluorescence and microscopy studies, with the help of MarB; MaxB and NN performed image analyses and statistical analyses. FR and CF performed the zebrafish experiments; MaxB, FR and CF analyzed and quantified images from zebrafish motoneurons and made statistics; AVK performed molecular modeling and suggested artificial TRIO mutants; SS and AD supervised the project and coordinated the study, in collaboration with DB; SS, AD, MaxB and CF wrote the manuscript. All authors reviewed and approved the manuscript.

COMPETING INTERESTS

The authors declare no competing interests.

ADDITIONAL INFORMATION

Supplementary information The online version contains supplementary material available at https://doi.org/10.1038/s41380-023-01963-x.

Correspondence and requests for materials should be addressed to Anne Debant or Susanne Schmidt.